SANDIA REPORT
SAND2018-8736
Unlimited Release
Printed August 2018

Formulas For Plane Wave Coupling To A Transmission Line Above Ground With Terminating Loads

Larry K. Warne and Salvatore Campione

Prepared by
Sandia National Laboratories
Albuquerque, New Mexico 87185 and Livermore, California 94550

Sandia National Laboratories is a multimission laboratory managed and operated by National Technology and Engineering Solutions of Sandia, LLC, a wholly owned subsidiary of Honeywell International, Inc., for the U.S. Department of Energy's National Nuclear Security Administration under contract DE-NA0003525.

Issued by Sandia National Laboratories, operated for the United States Department of Energy by National Technology and Engineering Solutions of Sandia, LLC.

Available to DOE and DOE contractors from
U.S. Department of Energy
Office of Scientific and Technical Information
P.O. Box 62
Oak Ridge, TN 37831

Telephone: (865) 576-8401
Facsimile: (865) 576-5728
E-Mail: reports@osti.gov
Online ordering: http://www.osti.gov/scitech

Available to the public from
U.S. Department of Commerce
National Technical Information Service
5301 Shawnee Rd
Alexandria, VA 22312

Telephone: (800) 553-6847
Facsimile: (703) 605-6900
E-Mail: orders@ntis.gov
Online order: https://classic.ntis.gov/help/order-methods/

SAND2018-8736
Unlimited Release
Printed August 2018

Formulas For Plane Wave Coupling To A Transmission Line Above Ground With Terminating Loads

Larry K. Warne and Salvatore Campione
Electromagnetic Theory Dept.

Sandia National Laboratories
P. O. Box 5800
Albuquerque, NM 87185-1152

Abstract

This report considers plane wave coupling to a transmission line consisting of a wire above a conducting ground. Comparisons are made for the two types of available source models, along with a discussion about the decomposition of the line currents. Simple circuit models are constructed for the terminating impedances at the ends of the line including radiation effects. Results from the transmission line with these loads show good agreement with full wave simulations.

Intentionally Left Blank

Contents

Figures

Intentionally Left Blank

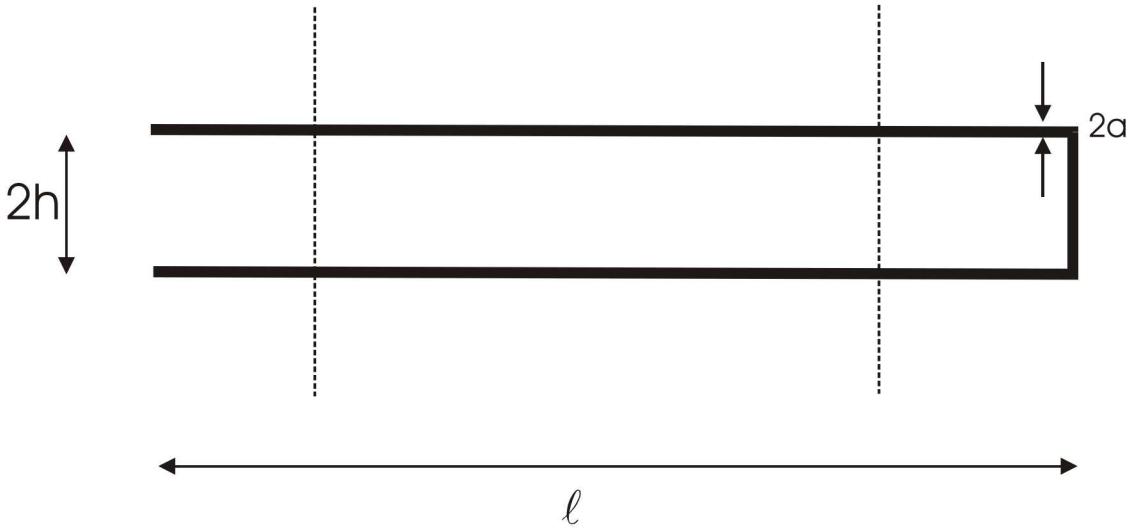

Figure 1. Geometry of transmission line with image for PEC ground..

1 INTRODUCTION

Our interest here is to examine transmission line models for a wire above a conductive half space. In particular, we are interested in lumped loads representing corrections to the distributed transmission line elements in order to approximately account for the fringe field corrections at the ends of the line under open circuit and short circuit terminations, as well as elements to account for radiation of the line.

We discuss and compare the two existing approaches for modeling plane wave field coupling to transmission lines in order to sort out the relevant sources and the associated meaning of the voltage and current solutions. We also discuss the different bases for the current decomposition (for example, transmission line and antenna modes).

The lumped capacitance and air conductance elements for an open circuit termination will have reasonably broad applicability since the distributed admittances of the transmission line model for dense lower dielectric half spaces are typically dominated by the air region above the conductive half space. The lumped inductance element for a short circuit termination will be somewhat approximate unless the skin depth in the conductive half space is small compared to the line height above the ground since we will use an image in the ground to describe the return current in this construction. Furthermore, the radiation elements are derived for a line with a reasonably concentrated image current, and are thus also limited to this small skin depth case. We note that for the large skin depth case, we expect the ground losses to dominate over the radiation losses, and furthermore, the damping may spread out resonant behavior in frequency to the point where the exact spectral position is less important. Nevertheless we include a short section briefly discussing the alternative approach of using the Wiener-Hopf reflection coefficient to treat both long lines and larger skin depths when the line end in an open circuit.

Figure 1 shows an example of a transmission line and its image in the conducting half space with "open" and "short" circuit loads.

2 TRANSMISSION LINE MODEL

A one-dimensional transmission line model is used here [1], [2], [3]. The transverse dimension is modeled in terms of cross sectional per unit length circuit parameters; we are primarily interested in the case of a wire above a finitely conducting ground, but will also touch on the two wire transmission line without ground (which can be an image in a perfectly conducting ground) in certain cases. The transmission line equations for time dependence $e^{-i\omega t}$, and appropriate per unit length immittances for a wire above a finitely conducting ground, are now listed [4], [5], [6], [7][8], [9]. The voltage equation is

$$\frac{dV}{dz} = E^{oc} - ZI \tag{1}$$

where the impedance per unit length is

$$Z = Z_w - i\omega L_e + Z_4 \tag{2}$$

with external inductance per unit length

$$L_e = L_2 + L_0 \tag{3}$$

and the wire dielectric coating inductance per unit length is

$$L_2 = \frac{\mu_0}{2\pi} \ln(b/a) \tag{4}$$

with air inductance per unit length above the ground plane

$$L_0 = \frac{\mu_0}{2\pi} \text{Arccosh}(h/b) \tag{5}$$

The current equation is

$$\frac{dI}{dz} = K^{sc} - YV \tag{6}$$

where the admittance per unit length is

$$1/Y = 1/Y_e + 1/Y_4 \tag{7}$$

with external admittance per unit length

$$1/Y_e = 1/(G_0 - i\omega C_0) + 1/(-i\omega C_2) \tag{8}$$

and wire dielectric coating capacitance per unit length

$$C_2 = \frac{2\pi\varepsilon_w}{\ln(b/a)} \tag{9}$$

with air capacitance per unit length C_0 and conductance per unit length G_0

$$C_0 + iG_0/\omega = \frac{2\pi\varepsilon}{\text{Arccosh}(h/b)} \tag{10}$$

and the ground parameters are taken as

$$Z_4 \approx -i\omega\mu_0 H_0^{(1)}(k_4 h) / \left[2\pi k_4 h H_1^{(1)}(k_4 h)\right] \approx -i\omega\frac{\mu_0}{2\pi}\ln\left(\frac{1-ik_4 h}{-ik_4 h}\right) \ , \ h > b \tag{11}$$

$$Y_4 \approx -i2\pi(\omega\varepsilon_4 + i\sigma_4) k_4 h H_1^{(1)}(k_4 h) / H_0^{(1)}(k_4 h) \approx -i2\pi(\omega\varepsilon_4 + i\sigma_4) / \ln\left(\frac{1-ik_4 h}{-ik_4 h}\right) \ , \ h > b \tag{12}$$

with ground propagation constant

$$k_4 = \sqrt{\omega\mu_0(\omega\varepsilon_4 + i\sigma_4)} \tag{13}$$

The external source terms are $E^{oc}(z)$ and $K^{sc}(z)$. For a plane wave at oblique incidence θ_0 with respect to the z axis we take these to have dependence

$$E^{oc} = E_0^{oc} e^{ikz\cos\theta_0} \tag{14}$$

$$K^{sc} = K_0^{sc} e^{ikz\cos\theta_0} \tag{15}$$

where

$$k = \omega\sqrt{\mu_0\varepsilon} \tag{16}$$

In this report we are focused on the case where the air conductivity is small enough that we can treat it as a damping effect along the transmission line, but not so large that it causes the air skin depth to become comparable to, or less than, the height of the transmission line above the ground; in the case where the air conductivity is large, the terminating load effects discussed here are probably not important due to the large line losses, and the fact that the line is significantly changed from the case where it is interacting with the ground. The impedance per unit length of the wire at high frequencies is

$$Z_w \sim Z_s / (2\pi a) \tag{17}$$

where the surface impedance of the metal is

$$Z_s = (1-i) R_s \tag{18}$$

the surface resistance is

$$R_s = 1/(\sigma\delta) \tag{19}$$

and the skin depth is

$$\delta = \sqrt{2/(\omega\mu\sigma)} \tag{20}$$

where the metal magnetic permeability is μ and the metal electric conductivity is σ. The complex permittivity of the air is taken as

$$\varepsilon = \varepsilon' + i\varepsilon'' = \varepsilon' + i\sigma_0/\omega \tag{21}$$

Elimination of the voltage in the transmission line equations gives

$$\left(\frac{d^2}{dz^2}+k_L^2\right)I=\frac{d}{dz}K^{sc}-YE^{oc}=\left(K_0^{sc}ik\cos\theta_0-YE_0^{oc}\right)e^{ikz\cos\theta_0} \tag{22}$$

where the propagation constant along the line is

$$k_L=\sqrt{-ZY} \tag{23}$$

and the characteristic impedance of the line is

$$Z_c=\sqrt{Z/Y} \tag{24}$$

The homogeneous equation is

$$\left(\frac{d^2}{dz^2}+k_L^2\right)I=0 \tag{25}$$

The general solution can be written as the sum of the particular solution and homogeneous solutions

$$I\left(z\right)=I_+e^{ik_Lz}+I_-e^{-ik_Lz}+I_p\left(z\right) \tag{26}$$

where $I_\pm$ are constants and $I_p\left(z\right)$ is a particular solution

$$I_p\left(z\right)=\left(\frac{K_0^{sc}ik\cos\theta_0-YE_0^{oc}}{k_L^2-k^2\cos^2\theta_0}\right)e^{ikz\cos\theta_0} \tag{27}$$

2.1 Transmission Line Mode - Antenna Mode Decomposition

If we consider a two wire line there are in general two distinct currents associated with the two wires. We can group these currents in various ways (choice of bases). One way is to group these two currents is in terms of a differential mode (two equal and oppositely directed currents) and a common mode (two equal currents in the same direction). However, if the two wires are asymmetrical (for example, different wire radii) there is coupling between these two modes [10]. Here we will instead choose to regard the bases as a transmission line mode with no net current (two equal and oppositely directed currents) and an antenna mode with zero voltage between wires [11]. In the perfectly conducting wire case the antenna mode currents are chosen so that the inductive voltage drops along the line wires are the same and there is no net voltage between wires along the line. If the two wires are not perfectly conducting, the internal impedance (including resistance) per unit length can be brought into the total series impedances per unit length to determine the antenna mode current in order to assure that there is no voltage difference between wires along the line; even with this internal impedance (and resistance) there is still no coupling between these modes and they can be treated independently. Consequently, we will focus on the independent transmission line mode, with a voltage difference between wires, in this report. Note that discontinuities in impedance along the line, which do not maintain the same voltages on the two wires (such as a lumped load in one of the wires and not the other at some point along the line) will lead to coupling between modes at the discontinuity.

2.2 Conventional Model And End Terminations

There are two distinct models for plane wave drives of transmission lines. The first is usually referred to as the conventional model (although here we also add the drives at the loads on the ends of the line). The conventional transmission line model uses the electric field component along the line conductors as a

drive. To be complete we also require the transverse electric field drive along the transverse load directions at both ends of the line. For the two-wire line along the z axis the distributed sources are a distributed open circuit voltage source equal to the difference between the incident axial drive field at the centroids of current (when driven in a differential mode) in the two conductors (the positive wire reference minus the negative wire reference)

$$E^{oc} = E_0^{oc} e^{ikz\cos\theta_0} = E_z^{inc}(h_e) - E_z^{inc}(-h_e) \tag{28}$$

and no distributed short circuit current source

$$K^{sc} = K_0^{sc} e^{ikz\cos\theta_0} = 0 \tag{29}$$

where for two circular wires of radius a and spacing $2h$ we note that $h_e = \sqrt{h^2 - a^2}$. We note that the sign of the distributed voltage source in the transmission line equation means that the we are actually imposing a distributed electric field source in the line which opposes the incident field (scattered field).

For a finite line over $0 \le z \le \ell$ with a load Z_1 at $z = 0$ and Z_2 at $z = \ell$ we impose the boundary conditions

$$V(0) = V_0(0) - Z_1 I(0) \tag{30}$$

$$V(\ell) = V_0(\ell) + Z_2 I(\ell) \tag{31}$$

where the transverse sources are

$$V_0(z) = \int_{C_{h_e}} \underline{E}^{inc} \cdot \underline{d\ell} = 2\underline{h}_e \cdot \underline{E}^{inc} \tag{32}$$

the path C_{h_e} starts on the negative reference conductor and proceeds to the positive reference conductor along the center of the load, and the vector $2\underline{h}_e$ points from the negative to positive reference conductor along the load. Note again that this end voltage source opposes the incident field (scattered field).

Taking the x axis to point from the negative to positive line conductors and an incident plane wave with electric field and wavenumber in the $x - z$ plane we can write the fields as

$$H_y^{inc} = H_0 e^{ikz\cos\theta_0 - ikx\sin\theta_0} = (E_0/\eta_0) e^{ikz\cos\theta_0 - ikx\sin\theta_0} \tag{33}$$

$$E_z^{inc} = \frac{1}{-i\omega\varepsilon_0}\frac{\partial}{\partial x} H_y^{inc} = E_0 \sin\theta_0 e^{ikz\cos\theta_0 - ikx\sin\theta_0} \tag{34}$$

$$E_x^{inc} = \frac{1}{i\omega\varepsilon_0}\frac{\partial}{\partial z} H_y^{inc} = E_0 \cos\theta_0 e^{ikz\cos\theta_0 - ikx\sin\theta_0} \tag{35}$$

Then the drive field is

$$E_z^{inc}(x = h_e) - E_z^{inc}(x = -h_e) \approx \lim_{x\to 0}\left[2h_e \frac{\partial}{\partial x} E_z^{inc}\right]$$

$$= \lim_{x\to 0}\left[-ik2h_e E_0 \sin^2\theta_0 e^{ikz\cos\theta_0 - ikx\sin\theta_0}\right] = -ik2h_e E_0 \sin^2\theta_0 e^{ikz\cos\theta_0} \tag{36}$$

At the loads

$$V_0(z) \approx 2h_e E_0 \cos\theta_0 e^{ikz\cos\theta_0} = -V_t^{inc}(z) \tag{37}$$

where the actual voltage created across the line by the incident field is V_t, but we are imposing minus this value (the scattered voltage). The solution for the current distribution in this problem is

$$\frac{Z_c I}{2h_e E_0} = \frac{Z_c}{2h_e E_0}\left(I_+ e^{ik_L z} + I_- e^{-ik_L z}\right) + \frac{kk_L \sin^2\theta_0}{k_L^2 - k^2\cos^2\theta_0} e^{ikz\cos\theta_0} \tag{38}$$

and the voltage distribution is

$$\frac{V}{2h_e E_0} = \frac{Z_c}{2h_e E_0}\left(I_+ e^{ik_L z} - I_- e^{-ik_L z}\right) + \frac{k^2 \sin^2\theta_0}{k_L^2 - k^2\cos^2\theta_0}\cos\theta_0 e^{ikz\cos\theta_0} \tag{39}$$

with line characteristic impedance and wavenumber (in this and the next two subsections we are limiting the insulator around the wires to the lossless case but not necessarily free space)

$$Z_c = \sqrt{L/C} \tag{40}$$

$$k_L = \omega\sqrt{LC} \tag{41}$$

where the two constants $I_\pm$ are

$$\pm\frac{Z_c I_\pm}{2h_e E_0} =$$

$$\frac{\left(k_L^2 - k^2\right)\left[\left(Z_c \pm Z_2\right) - \left(Z_c \mp Z_1\right)e^{ik\ell\cos\theta_0 \pm ik_L\ell}\right] Z_c\cos\theta_0 - \left[\left(Z_c \pm Z_2\right)Z_1 + \left(Z_c \mp Z_1\right)Z_2 e^{ik\ell\cos\theta_0 \pm ik_L\ell}\right] k_L k \sin^2\theta_0}{\left(k_L^2 - k^2\cos^2\theta_0\right)\left[\left(Z_c \pm Z_1\right)\left(Z_c \pm Z_2\right) - \left(Z_c \mp Z_1\right)\left(Z_c \mp Z_2\right)e^{\pm i2k_L\ell}\right]} \tag{42}$$

2.3 Dual Source Model

The second model for plane wave drives of transmission lines we refer to as the dual source model [10]. The dual source model uses the transverse magnetic and electric field components between the line conductors as drives. For the two-wire line the sources include the transverse scattered field so that the sum of the two fields satisfies the wire surface boundary conditions [10] (this sum does not include the TEM mode part of the field [10])

$$E^{oc} = E_0^{oc} e^{ikz\cos\theta_0} = i\omega\int_{C_{h_e}}\left(\underline{B}^{inc} + \underline{B}^{scatt}\right)\cdot\underline{n}d\ell = i\omega\int_{C_{h_e}}\left(\underline{B}^{inc} + \underline{B}^{scatt}\right)\cdot\left(\underline{d\ell}\times\underline{e}_z\right)$$

$$= i\omega\left(2\underline{h}_e\times\underline{e}_z\right)\cdot\underline{B}^{inc} = i\omega\mu_0\left(\underline{n}\cdot\underline{H}^{inc}\right)2h_e = -i\omega\mu_0 H_0 e^{ikz\cos\theta_0}2h_e \tag{43}$$

$$K^{sc} = K_0^{sc} e^{ikz\cos\theta_0} = i\omega C\int_{C_{h_e}}\left(\underline{E}^{inc} + \underline{E}^{scatt}\right)\cdot\underline{d\ell}$$

$$= i\omega C 2\underline{h}_e \cdot \underline{E}^{inc} = i\omega C \underline{E}^{inc} \cdot (\underline{e}_z \times \underline{n})\, 2h_e = i\omega C E_0 2h_e \cos\theta_0 e^{ikz\cos\theta_0} \tag{44}$$

At the ends of the line we impose the boundary conditions

$$V(0) = -Z_1 I(0) \tag{45}$$

$$V(\ell) = Z_2 I(\ell) \tag{46}$$

Solution of the this problem is identical to the current in the conventional approach (38) with coefficients (42), but the voltage is

$$\frac{V}{2h_e E_0} = \frac{Z_c}{2h_e E_0}\left(I_+ e^{ik_L z} - I_- e^{-ik_L z}\right) + \frac{k^2 \sin^2\theta_0}{k_L^2 - k^2\cos^2\theta_0}\cos\theta_0 e^{ikz\cos\theta_0} - \cos\theta_0 e^{ikz\cos\theta_0} \tag{47}$$

or

$$V_{dual} = V_{conv} - V_0 = V_{conv} + V_t^{inc} \tag{48}$$

Hence, the conventional approach (including end sources) provides the same current but only the scattered part of the transverse voltage, whereas, the dual source approach provides the same current but the total voltage (including the incident field transverse voltage).

2.4 Limiting Cases of Two Wire Model Results

Some limiting cases of the line voltage make this more clear (the line current for the two cases already agree). For simplicity we take $Z_2 = Z_1$. First, taking $k\ell\cos\theta_0 << 1$ and $k_L\ell << 1$ we find

$$\pm\frac{Z_c I_\pm}{2h_e E_0} \sim \frac{\left(k_L^2 - k^2\right)\cos\theta_0 \mp k_L k \sin^2\theta_0}{2\left(k_L^2 - k^2\cos^2\theta_0\right)} \tag{49}$$

$$V_{conv} \sim 2h_e E_0 \cos\theta_0 \sim -V_t^{inc} \tag{50}$$

$$V_{dual} \to 0 \tag{51}$$

The transmission line separation between conductors is assumed to be electrically small to begin with, so the end loads Z_1 short out the field. The dual source voltage limit shows this, whereas, the conventional source voltage limit produces negative the incident transverse voltage (the scattered transverse voltage). Secondly, if we first take $Z_1/Z_c \to \infty$, and then assume that $k\ell\cos\theta << 1$ and $k_L\ell << 1$

$$\frac{Z_c I_\pm}{2h_e E_0} \sim -\frac{k\sin^2\theta_0}{2\left(k_L \mp k\cos\theta_0\right)} \tag{52}$$

The voltage then becomes

$$V_{conv} \to 0 \tag{53}$$

$$V_{dual} \sim -2h_e E_0 \cos\theta_0 \sim V_t^{inc} \tag{54}$$

In this case we have first eliminated the end loads in the limit $Z_1/Z_c \to \infty$, so we expect the electrically short line to reproduce the incident transverse voltage. The dual source voltage limit shows this, whereas, the conventional source voltage limit vanishes (the scattered transverse voltage).

Both methods are valid but they produce different results depending on whether the incident transverse voltage is included or not. Note also that the conventional method boundary conditions (30) and (31) in the special case of open circuit conditions $Z_1, Z_2 \to \infty$ imply that $I(0) = 0 = I(\ell)$, independent of the end sources $V_0(z)$; however, with the higher-order end load C_t discussed below, this source has some effect even under nominal open circuit conditions!

2.5 Ground Plane Case

If we consider the case where a ground plane is inserted into the two wire transmission line of the preceding subsections, the impedance (inductance) per unit length and the characteristic impedance Z_c is cut in half, the admittance (capacitance) per unit length doubles. The sources E^{oc}, K^{sc}, V_0 (and V_t) are left unchanged because the path length is cut in half ($2h_e$ is replaced by h_e), but the reflected plane wave from the surface doubles the tangential magnetic and normal electric drive fields. Thus the voltage is left unchanged but the current doubles.

For a finitely conducting ground half space there will be added contributions to the impedance and to the admittance as well as modifications to the reflected part of the drive fields. Nevertheless, because the line voltage is largely supported by the air region above the ground plane, we expect that in the conventional method the incident (and reflected) transverse voltage must be added to the transmission line voltage to obtain the total voltage. The incident plus reflected plane wave fields (with zero phase reference on the plane interface at $x = 0$) can be written as

$$H_y^{inc} + H_y^{ref} = H_0 \left(e^{-ikx\sin\theta_0} + R_H e^{ikx\sin\theta_0}\right) e^{ikz\cos\theta_0} = (E_0/\eta_0)\left(e^{-ikx\sin\theta_0} + R_H e^{ikx\sin\theta_0}\right) e^{ikz\cos\theta_0} \tag{55}$$

$$E_z^{inc} + E_z^{ref} = \frac{1}{-i\omega\varepsilon_0}\frac{\partial}{\partial x}\left(H_y^{inc} + H_y^{ref}\right) = E_0\sin\theta_0\left(e^{-ikx\sin\theta_0} - R_H e^{ikx\sin\theta_0}\right) e^{ikz\cos\theta_0} \tag{56}$$

$$E_x^{inc} + E_x^{ref} = \frac{1}{i\omega\varepsilon_0}\frac{\partial}{\partial z}\left(H_y^{inc} + H_y^{ref}\right) = E_0\cos\theta_0\left(e^{-ikx\sin\theta_0} + R_H e^{ikx\sin\theta_0}\right) e^{ikz\cos\theta_0} \tag{57}$$

where the TM reflection coefficient is

$$R_H = \frac{(k_4/k)^2\sin\theta_0 - \sqrt{(k_4/k)^2 - \cos^2\theta_0}}{(k_4/k)^2\sin\theta_0 + \sqrt{(k_4/k)^2 - \cos^2\theta_0}} \tag{58}$$

The distributed voltage source in the conventional method is then (note that the fields vanish deep in the ground so the contribution to the source from this region vanishes)

$$E^{oc} = E_0^{oc} e^{ikz\cos\theta_0} = E_z^{inc}(h_e) + E_z^{ref}(h_e) = E_0\sin\theta_0\left(e^{-ikh_e\sin\theta_0} - R_H e^{ikh_e\sin\theta_0}\right) e^{ikz\cos\theta_0} = A_0 e^{ikz\cos\theta_0} \tag{59}$$

with no distributed short circuit current source, but end transverse sources

$$V_0(z) \approx h_e\left[E_x^{inc}(h_e) + E_x^{ref}(h_e)\right] \approx 2h_e E_0 \cos\theta_0 \left(e^{-ikh_e \sin\theta_0} + R_H e^{ikh_e \sin\theta_0}\right) e^{ikz\cos\theta_0} = -V_t^{inc}(z) \quad (60)$$

3 SHORT CIRCUIT INDUCTIVE TERMINATION

The procedure [12] is to use a formula for the static inductance of a rectangular loop. One half this value is differenced by subtraction of the inductance per unit length of a two wire transmission line times the length. This difference forms the estimate for the terminating inductance of the "shorted" end of the resonator. Using Grover [13] for the inductance of a rectangular loop of perfectly conducting wire with small radius a and dimensions 2ℓ and $2h$

$$L_{loop} =$$

$$\frac{\mu_0}{\pi}\left[2h\ln(4h/a) + 2\ell\ln(4\ell/a) + 2\sqrt{4h^2+4\ell^2} - 2h\text{Arcsinh}\left(\frac{h}{\ell}\right) - 2\ell\text{Arcsinh}(\ell/h) - 2(2h+2\ell)\right],\ 2\ell, 2h >> a \quad (61)$$

We approximate with $2\ell >> 2h$

$$L_{loop} \sim \frac{\mu_0}{\pi}\left[2h\ln(4h/a) + 2\ell\ln(2h/a) - 4h\right],\ 2\ell >> 2h >> a \quad (62)$$

Taking one half this inductance for the half loop and subtracting the transmission line inductance per unit length (note that $L \approx L_e$ since an insulation coating on the wire usually has the permeability of free space)

$$L = \frac{\mu_0}{\pi}\text{Arccosh}\left(\frac{h}{a}\right) \sim \frac{\mu_0}{\pi}\ln(2h/a),\ 2h >> 2a \quad (63)$$

times ℓ

$$L_t = \frac{1}{2}L_{loop} - \ell L \sim 2h\frac{\mu_0}{2\pi}\left[\ln(4h/a) - 2\right] \quad (64)$$

In our case it may be more consistent (and slightly more accurate) to replace h by h_e in these formulas. Now for the wire above a PEC plane we take one half this value for the end load inductance of the short circuits

$$L_t^{GP} \sim h\frac{\mu_0}{2\pi}\left[\ln(4h/a) - 2\right] \quad (65)$$

$$L^{GP} = \frac{\mu_0}{2\pi}\text{Arccosh}\left(\frac{h}{a}\right) \sim \frac{\mu_0}{2\pi}\ln(2h/a),\ 2h >> 2a \quad (66)$$

When the down conductor has loss the terminating impedance is

$$Z_t^{GP} = Z_w h - i\omega L_t^{GP} \quad (67)$$

For a finitely conducting half space this will also hold for small skin depth compared to the line height, provided we add a terminating load at the interface, which is discussed below.

4 OPEN CIRCUIT CAPACITIVE TERMINATION

The procedure [12] is to estimate the static capacitance of a long or semi-infinite two wire line charged to a potential difference. In this section we take the permittivity of the air ε to be real; if it is complex we can either replace ε by the real part ε' or use the complex permittivity $\varepsilon = \varepsilon' + i\varepsilon'' = \varepsilon' + i\sigma_0/\omega$ but replace the capacitance C by the combination $C + iG/\omega$; we also ignore the presence of an insulation layer and replace b by a in this section. The iterative procedure is a static version of that used to solve the problem of a thin cylindrical antenna [14]. The two conductor capacitance per unit length, times the length, is subtracted to yield the terminating capacitance of the "open" end of the resonator. The potential is (we use the thin wire kernel here)

$$\phi = \frac{1}{4\pi\varepsilon}\int_0^\ell \left[\frac{1}{\sqrt{\rho_+^2 + (z-z')^2}} - \frac{1}{\sqrt{\rho_-^2 + (z-z')^2}}\right] q(z')\, dz' \tag{68}$$

where

$$\rho_\pm = \sqrt{(x \mp h)^2 + y^2} \tag{69}$$

The integral equation for the charge density is then found by setting $\phi = \pm V/2$ on the wire surface. We let $\ell \to \infty$

$$2\pi\varepsilon V = \int_0^\infty \left[\frac{1}{\sqrt{a^2 + (z-z')^2}} - \frac{1}{\sqrt{4h^2 + (z-z')^2}}\right] q(z')\, dz' \tag{70}$$

Now to develop an approximate solution we first write

$$2\pi\varepsilon V = q(z)\int_0^\infty \left[\frac{1}{\sqrt{a^2 + (z-z')^2}} - \frac{1}{\sqrt{4h^2 + (z-z')^2}}\right] dz'$$

$$+ \int_0^\infty \left[\frac{1}{\sqrt{a^2 + (z-z')^2}} - \frac{1}{\sqrt{4h^2 + (z-z')^2}}\right] [q(z') - q(z)]\, dz' \tag{71}$$

Using

$$\int_0^\ell \frac{dz'}{\sqrt{a^2 + (z-z')^2}} = \text{Arcsinh}\left(\frac{\ell - z}{a}\right) + \text{Arcsinh}\left(\frac{z}{a}\right) \tag{72}$$

gives

$$2\pi\varepsilon V = q(z)\left[\ln(2h/a) - \text{Arcsinh}(z/(2h)) + \text{Arcsinh}(z/a)\right]$$

$$+ \int_0^\infty \left[\frac{1}{\sqrt{a^2 + (z-z')^2}} - \frac{1}{\sqrt{4h^2 + (z-z')^2}}\right] [q(z') - q(z)]\, dz' \tag{73}$$

For small a we can write this as

$$2\pi\varepsilon V \sim \Omega q\left(z\right) - q\left(z\right)\left[\ln\left\{z/\left(2h\right) + \sqrt{z^2/\left(2h\right)^2 + 1}\right\} - \ln\left(z/h\right)\right]$$

$$+ \int_0^\infty \left[\frac{1}{|z - z'|} - \frac{1}{\sqrt{4h^2 + \left(z - z'\right)^2}}\right]\left[q\left(z'\right) - q\left(z\right)\right] dz' \tag{74}$$

where we define

$$\Omega = 2\ln\left(2h/a\right) \tag{75}$$

An iterative solution is obtained by assuming Ω is large

$$q\left(z\right)/V \sim \frac{2\pi\varepsilon}{\Omega}\left[1 + \frac{1}{\Omega}\left\{\ln\left(z/\left(2h\right) + \sqrt{z^2/\left(2h\right)^2 + 1}\right) - \ln\left(z/h\right)\right\}\right.$$

$$+\frac{1}{\Omega^2}\left\{\ln\left(z/\left(2h\right) + \sqrt{z^2/\left(2h\right)^2 + 1}\right) - \ln\left(z/h\right)\right\}^2$$

$$-\frac{1}{\Omega^2}\int_0^\infty \left\{\frac{1}{|z - z'|} - \frac{1}{\sqrt{4h^2 + \left(z - z'\right)^2}}\right\}\left\{\ln\left(\frac{z'/\left(2h\right) + \sqrt{z'^2/\left(2h\right)^2 + 1}}{z/\left(2h\right) + \sqrt{z^2/\left(2h\right)^2 + 1}}\right) - \ln\left(z'/z\right)\right\} dz'$$

$$\left. + \cdots\right] \tag{76}$$

The leading term is the transmission line capacitance per unit length

$$q_0/V = C \tag{77}$$

where

$$C = \frac{\pi\varepsilon}{\mathrm{Arccosh}\left(h/a\right)} \sim \frac{\pi\varepsilon}{\ln\left(2h/a\right)}\ ,\ 2h >> 2a \tag{78}$$

The next term can be integrated to give the leading terminating capacitance

$$C_t \sim \frac{2\pi\varepsilon}{\Omega^2}\int_0^\infty \left\{\ln\left(z/\left(2h\right) + \sqrt{z^2/\left(2h\right)^2 + 1}\right) - \ln\left(z/h\right)\right\} dz$$

$$\sim \frac{4\pi h\varepsilon}{\Omega^2}\int_0^\infty \left\{\ln\left(u + \sqrt{u^2 + 1}\right) - \ln\left(2u\right)\right\} du \tag{79}$$

Letting

$$u + \sqrt{u^2 + 1} = s \tag{80}$$

$$\frac{1}{2}\left(s - 1/s\right) = u \tag{81}$$

$$du = \frac{1}{2}\left(1 + 1/s^2\right) ds \tag{82}$$

gives

$$C_t \sim \frac{4\pi h\varepsilon}{\Omega^2} \lim_{U\to\infty} \left[\frac{1}{2} \int_1^{U+\sqrt{U^2+1}} \ln(s) \left(1 + 1/s^2\right) ds - U\left\{\ln(2U) - 1\right\} \right] \tag{83}$$

Using

$$\int_1^{U+\sqrt{U^2+1}} \ln(s) \left(1 + 1/s^2\right) ds =$$

$$\left(U + \sqrt{U^2+1}\right) \left\{ \ln\left(U + \sqrt{U^2+1}\right) - 1 \right\} + 1 - \left(U + \sqrt{U^2+1}\right)^{-1} \left\{ \ln\left(U + \sqrt{U^2+1}\right) + 1 \right\} + 1 \tag{84}$$

gives

$$C_t \sim \frac{4\pi h\varepsilon}{\Omega^2} \tag{85}$$

To include the next term we write it as

$$C_t \sim \frac{4\pi h\varepsilon}{\Omega^2} \left(1 + C_1/\Omega\right) \tag{86}$$

where

$$hC_1 \sim \int_0^\infty \left\{ \ln\left(z/(2h) + \sqrt{z^2/(2h)^2 + 1} \right) - \ln(z/h) \right\}^2 dz$$

$$- \int_0^\infty \int_0^\infty \left\{ \frac{1}{|z - z'|} - \frac{1}{\sqrt{4h^2 + (z - z')^2}} \right\} \left\{ \ln\left(\frac{z'/(2h) + \sqrt{z'^2/(2h)^2 + 1}}{z/(2h) + \sqrt{z^2/(2h)^2 + 1}} \right) - \ln(z'/z) \right\} dz'dz \tag{87}$$

or

$$C_1 \sim \int_0^\infty \left\{ \ln\left(u + \sqrt{u^2+1}\right) - \ln(2u) \right\}^2 du$$

$$- \int_0^\infty \int_0^\infty \left\{ \frac{1}{|u - u'|} - \frac{1}{\sqrt{1 + (u - u')^2}} \right\} \left\{ \ln\left(\frac{u' + \sqrt{u'^2+1}}{u + \sqrt{u^2+1}} \right) - \ln(u'/u) \right\} du'du \tag{88}$$

Carrying the first of these out using integration by parts

$$\int_0^U \left\{ \ln\left(u + \sqrt{u^2+1}\right) - \ln(2u) \right\}^2 du = \left\{ \ln\left(U + \sqrt{U^2+1}\right) - \ln(2U) \right\}^2 U$$

$$-2\int_0^U \left\{\ln\left(u+\sqrt{u^2+1}\right)-\ln(2u)\right\}\left(\frac{u}{\sqrt{u^2+1}}-1\right)du$$

$$=\left\{\ln\left(U+\sqrt{U^2+1}\right)-\ln(2U)\right\}^2 U$$

$$-2\left\{\ln\left(U+\sqrt{U^2+1}\right)-\ln(2U)\right\}\left(\sqrt{U^2+1}-U-1\right)$$

$$+2\int_0^U \left(\frac{1}{\sqrt{u^2+1}}-\frac{1}{u}\right)\left(\sqrt{u^2+1}-u-1\right)du$$

$$=\left\{\ln\left(U+\sqrt{U^2+1}\right)-\ln(2U)\right\}^2 U$$

$$-2\left\{\ln\left(U+\sqrt{U^2+1}\right)-\ln(2U)\right\}\left(\sqrt{U^2+1}-U-1\right)$$

$$+2\int_0^U \left\{2-\frac{2u}{\sqrt{u^2+1}}-\frac{1}{\sqrt{u^2+1}}-\frac{1}{u\sqrt{u^2+1}}+\frac{1}{u}\right\}du$$

$$=\left\{\ln\left(U+\sqrt{U^2+1}\right)-\ln(2U)\right\}^2 U$$

$$-2\left\{\ln\left(U+\sqrt{U^2+1}\right)-\ln(2U)\right\}\left(\sqrt{U^2+1}-U-1\right)$$

$$+2\left\{2U-2\sqrt{U^2+1}-\operatorname{Arcsinh}(U)+\ln\left(1+\sqrt{U^2+1}\right)+2-\ln 2\right\} \tag{89}$$

In the limit $U\to\infty$

$$\int_0^\infty \left\{\ln\left(u+\sqrt{u^2+1}\right)-\ln(2u)\right\}^2 du = 4(1-\ln 2) \tag{90}$$

Using the symmetry

$$\int_0^\infty\int_0^\infty \left\{\frac{1}{\sqrt{\nu^2+(u-u')^2}}-\frac{1}{\sqrt{1+(u-u')^2}}\right\}\left\{\ln\left(u'+\sqrt{u'^2+1}\right)-\ln(2u')\right\}du'du$$

$$=\int_0^\infty\int_0^\infty \left\{\frac{1}{\sqrt{\nu^2+(u-u')^2}}-\frac{1}{\sqrt{1+(u-u')^2}}\right\}\left\{\ln\left(u+\sqrt{u^2+1}\right)-\ln(2u)\right\}du'du \tag{91}$$

and noting that

$$\int_0^U \left\{\frac{1}{\sqrt{\nu^2+(u-u')^2}}-\frac{1}{\sqrt{1+(u-u')^2}}\right\}du'$$

$$= \text{Arcsinh}\left(\frac{U-u}{\nu}\right) + \text{Arcsinh}\left(\frac{u}{\nu}\right) - \text{Arcsinh}\left(U-u\right) + \text{Arcsinh}\left(u\right) \tag{92}$$

$$\int_0^\infty \left\{ \frac{1}{\sqrt{\nu^2 + \left(u-u'\right)^2}} - \frac{1}{\sqrt{1 + \left(u-u'\right)^2}} \right\} du' = -\ln\nu + \text{Arcsinh}\left(\frac{u}{\nu}\right) + \text{Arcsinh}\left(u\right)$$

$$\sim 2\ln\left(2u/\nu\right)\ ,\ u \to \infty \tag{93}$$

we see that the integrals are convergent. The difference of the two sides shows that the second integral vanishes. Note that the limit $\nu \to 0$, after the difference of the two sides is taken, produces the required absolute value. Thus

$$C_1 = 4\left(1 - \ln 2\right) \tag{94}$$

and finally

$$C_t \sim 2hC\frac{1}{\Omega}\left[1 + 4\left(1-\ln 2\right)/\Omega\right] \tag{95}$$

$$C \sim 2\pi\varepsilon/\Omega \tag{96}$$

$$\Omega = 2\ln\left(2h/a\right) \tag{97}$$

A numerical calculation with $\ell = 5$ m, $2h = 0.3$ m, $a = 0.03$ m gives $C_t = \varepsilon\left(0.110\text{ m}\right)$ whereas the formula gives $C_t = \varepsilon\left(0.11257\text{ m}\right)$. This is an error of only 2.3%. Larger aspect ratios h/a are expected to be even more accurate. In our case it may be more consistent (and slightly more accurate) to replace h by h_e in these formulas.

For the case of the wire above a PEC ground plane (since the air region typically dominates the admittance elements for a finitely conducting, but electrically dense conductive half space, these will also approximately hold for the finitely conducting half space)

$$C_t^{GP} \sim 2hC^{GP}\frac{1}{\Omega}\left[1 + 4\left(1-\ln 2\right)/\Omega\right] \tag{98}$$

$$C^{GP} \sim 4\pi\varepsilon/\Omega \tag{99}$$

$$\Omega = 2\ln\left(2h/a\right) \tag{100}$$

The case where $a = 0.5$ in and $h = 10$ m gives $C^{GP} = \varepsilon\left(0.853475\right)$ and $C_t^{GP} = \varepsilon\left(1.25596\text{ m}\right)$. The case where $a = 0.37$ in and $h = 1.5$ m gives $C^{GP} = \varepsilon\left(1.08972\right)$ and $C_t = \varepsilon\left(0.3136666\text{ m}\right)$.

Now inserting the complex permittivity the terminating admittance can be taken as

$$Y_t^{GP} = G_t^{GP} - i\omega C_t^{GP} \sim -i\omega 2h\frac{4\pi\varepsilon}{\Omega^2}\left[1 + 4\left(1-\ln 2\right)/\Omega\right] \tag{101}$$

with admittance per unit length

$$Y^{GP} = G^{GP} - i\omega C^{GP} \sim -i\omega 4\pi\varepsilon/\Omega \tag{102}$$

5 COMPARISON OF CST SIMULATIONS WITH ATLOG

This section compares full wave simulations of transmission lines above a perfectly conducting ground using CST Microwave Studio software, with calculations using the transmission line equations labeled as ATLOG (Analytic Transmission Line Over Ground) [9]. All these comparisons are for the case of normal incidence and use a simple unit electric field amplitude sine-squared pulse of 200 ns duration. The line has height $h = 5$ m and a radius of $a = 1$ cm (there is no insulation coating and the wire is a perfect conductor). Line lengths of 20 m, 40 m, 60 m, 80 m, and 100 m are shown. Both cases with open circuits at both ends of the line, as well as cases with down conductors (having the same radius as the line conductor) forming near short circuits at both ends of the line, are considered here.

Figure 2 shows simulations of a section of line with open circuits at both ends of the line. The dotted curves have idealized open circuits at the ends of the transmission line, whereas the solid curves have the preceding terminating capacitive loads. Notice that the phase shift caused by the terminating capacitive loads results in alignment of the curves in phase with the full wave simulations given by the dashed curves. Radiation damping is present in the full wave simulations as illustrated by the slight decay shown in the long dashed curve for the 20 m length.

Figure 3 shows simulations of a section of line with short circuits at both ends of the line. The dotted curves have idealized short circuits at the ends of the transmission line, whereas the solid curves have the preceding terminating inductive loads. Notice that the transmission line with idealized terminating short circuits shows no ringing and tracks the incident pulse used in these simulations. When the terminating inductances are added the response current rings due to the length of the line in agreement with the full wave simulations given by the dashed curves.

6 BASE PORT TERMINATION

We sometimes run into a case where the port is formed at the base of the transmission line near the ground plane. In such a case the "open circuit" capacitive load is modified by the down conductor.

6.1 Early Time Down-conductor Transmission Line

At early times the down conductor behaves as a transmission line. Using a biconical transmission line model with varying angle we can write these elements as approximately [1]

$$\psi(y) = \operatorname{arccot}(y/a) \tag{103}$$

$$L^{GP}(y) \approx \frac{\mu_0}{2\pi} \ln\left[\cot\left\{\psi(y)/2\right\}\right] \sim \frac{\mu_0}{2\pi} \ln(2y/a) \tag{104}$$

$$Z_i \sim Z_s/(2\pi a) \tag{105}$$

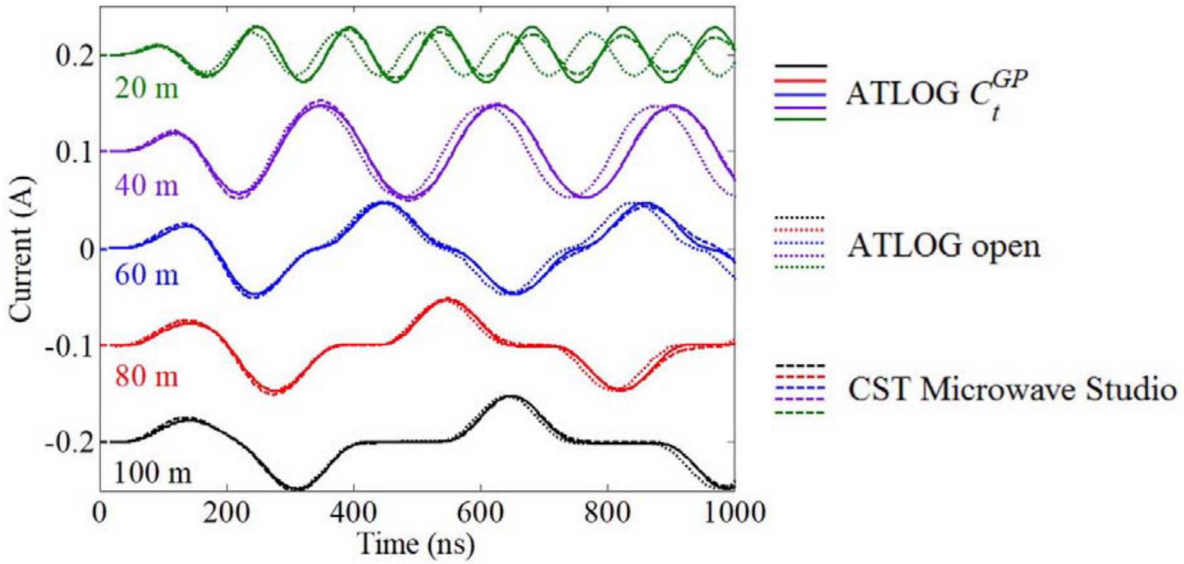

Figure 2. Comparison of full wave simulations (dashed curves) using CST Microwave Studio with transmission line having idealized open circuits at each end (dotted curves) and with a transmission line having terminating capacitors at each end (solid curves). The line lengths are given on the left end of the graph. Note that an arbitrary shift of ± 0.1 A has been added to the 40 m and 80 m length results, and an arbitrary shift of ± 0.2 A has been added to the 20 m and 100 m curves, to separate the different lengths and make the different curves readable.

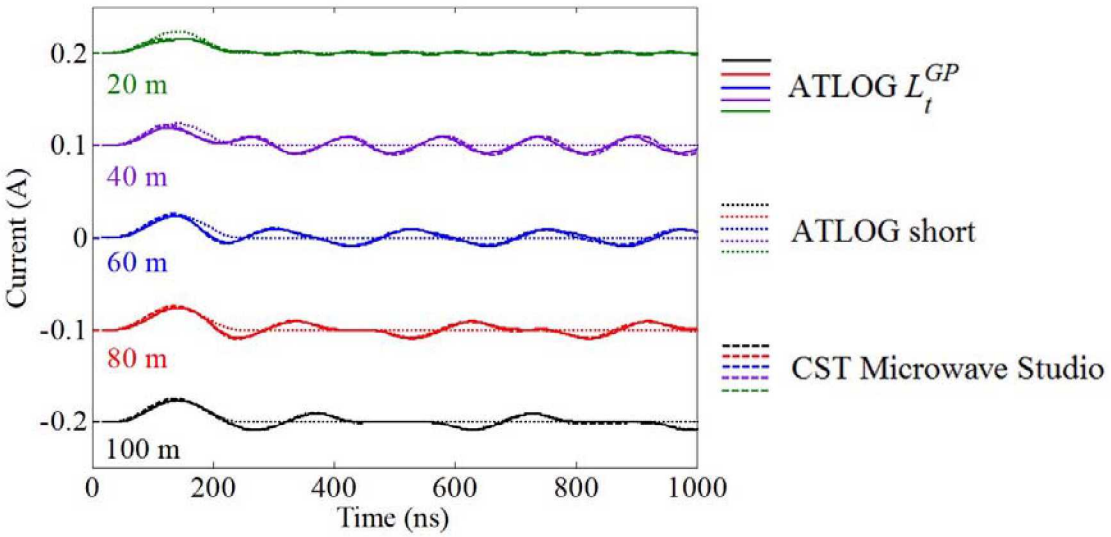

Figure 3. Comparison of full wave simulations (dashed curves) using CST Microwave Studio with transmission line having idealized short circuits at each end (dotted curves) and with a transmission line having terminating inductances at each end (solid curves). The line lengths are given on the left end of the graph. Note that an arbitrary shift of ± 0.1 A has been added to the 40 m and 80 m length results, and an arbitrary shift of ± 0.2 A has been added to the 20 m and 100 m curves, to separate the different lengths and make the different curves readable.

$$C^{GP}(y) \approx 2\pi\varepsilon'/\ln\left[\cot\left\{\psi(y)/2\right\}\right] \sim 2\pi\varepsilon'/\ln(2y/a) \tag{106}$$

$$G^{GP}(y) \approx 2\pi\sigma_0/\ln\left[\cot\left\{\psi(y)/2\right\}\right] \sim 2\pi\sigma_0/\ln(2y/a) \tag{107}$$

6.2 Open Circuit Lumped Capacitive Termination

The terminating element at later times for this case is

$$Y_t^{GP} = G_t^{GP} - i\omega C_t^{GP} + 1/\left(Z_{it} - i\omega L_t^{GP}\right) \tag{108}$$

where the impedance elements for this near open circuit condition are

$$Z_{it} \sim \frac{1}{3}\int_{h_p}^{h} Z_i dy \sim \frac{1}{3} Z_i (h - h_p) \tag{109}$$

$$L_t^{GP} \sim \frac{1}{3}\int_{h_p}^{h} L^{GP}(y)\, dy \approx \frac{1}{3}\frac{\mu_0}{2\pi}\left[(\Omega - 2)/2 + \ln(h/h_p)/(h/h_p - 1)\right](h - h_p) \tag{110}$$

Replacing the exact integration

$$\int_{h_p}^{h} \frac{dy}{\ln(2y/a)} = \frac{a}{2}\int_{2h_p/a}^{2h/a} \frac{du}{\ln u} = \frac{a}{2}\left[\mathrm{li}(2h/a) - \mathrm{li}(2h_p/a)\right] \tag{111}$$

in the admittance elements by the average approximation

$$\int_{h_p}^{h} \frac{dy}{\ln(2y/a)} = \frac{a}{2}\int_{2h_p/a}^{2h/a} \frac{du}{\ln u} \approx \frac{a}{2\langle \ln u\rangle}\int_{2h_p/a}^{2h/a} du = \frac{h - h_p}{\langle \ln u\rangle} \tag{112}$$

where

$$\langle \ln u\rangle = \int_{2h_p/a}^{2h/a} \ln u\, du \Big/ \int_{2h_p/a}^{2h/a} du = \left[(2h/a)\left\{\ln(2h/a) - 1\right\} - (2h_p/a)\left\{\ln(2h_p/a) - 1\right\}\right]\frac{a/2}{h - h_p}$$

$$= \ln(2h/a) + \frac{\ln(h/h_p)}{h/h_p - 1} - 1 = (\Omega - 2)/2 + \ln(h/h_p)/(h/h_p - 1) \tag{113}$$

we write these admittance circuit elements as

$$C_t^{GP} \sim \int_{h_p}^{h} C^{GP}(y)\, dy \approx \frac{2\pi\varepsilon'}{(\Omega - 2)/2 + \ln(h/h_p)/(h/h_p - 1)}(h - h_p) \tag{114}$$

$$G_t^{GP} \sim \int_{h_p}^{h} G^{GP}(y)\, dy \approx \frac{2\pi\sigma_0}{(\Omega - 2)/2 + \ln(h/h_p)/(h/h_p - 1)}(h - h_p) \tag{115}$$

In the case where the base height h_p approaches zero (order of radius a) these average results approach a finite limit since $\ln(h/h_p)/(h/h_p - 1) \to 0$. However, a correction is required for the base gap region when the gap dimension $g = O(a)$ [15]. For a solid cylinder of radius a and gap g to the ground plane we can

write these corrections to be added to the prior terminating capacitance and conductance elements as [15]

$$C_t^{GP} \to C_t^{GP} + \Delta C_t^{GP} \tag{116}$$

$$G_t^{GP} \to G_t^{GP} + \Delta G_t^{GP} \tag{117}$$

$$\Delta C_t^{GP} / \left(4a\varepsilon'\right) \approx \ln\left(\frac{\pi a}{2g}\right) + 1 - \gamma - 2/15 + \frac{\pi a}{2g} \tag{118}$$

$$\Delta G_t^{GP} / \left(4a\sigma_0\right) \approx \ln\left(\frac{\pi a}{2g}\right) + 1 - \gamma - 2/15 + \frac{\pi a}{2g} \tag{119}$$

where $\gamma \approx 0.5772$ is Euler's constant.

7 GROUND ROD TERMINATION

A ground rod termination into the conductive half space is often used in the "shorted" case. This implies that there is a series term that must be added to the perfectly conducting ground plane termination impedance Z_t^{GP}

$$Z_t^{GP} \to Z_t^{GP} + Z_r \tag{120}$$

Two cases are illustrated for the ground rod termination.

7.1 Low Conductivity Ground

If the ground conductivity is low, where the propagation decay length (or skin depth) is much larger than the ground rod length h_r, it is convenient to regard this term as a series admittance (we are ignoring the inductance and resistance of the ground rod here)

$$1/Z_r = Y_r = -i\left(\omega\varepsilon_4 + i\sigma_4\right)\frac{4\pi h_r}{\Omega_c} \tag{121}$$

$$\Omega_c = \Omega_r - 2\left(1 + \ln 2\right) \tag{122}$$

$$\Omega_r = 2\ln\left(2h_r/a_r\right) \tag{123}$$

7.2 High Conductivity Ground

In the case where the ground conductivity is high, such that the decay length is shorter than the ground rod length, we do not see the end of the ground rod, which is then treated as an antenna in the ground.

$$Z_4 = -i\omega\mu_0 H_0^{(1)}\left(k_4 a\right) / \left[2\pi k_4 a H_1^{(1)}\left(k_4 a\right)\right] \tag{124}$$

$$Y_4 = -i2\pi\left(\omega\varepsilon_4 + i\sigma_4\right) k_4 a H_1^{(1)}\left(k_4 a\right) / H_0^{(1)}\left(k_4 a\right) \tag{125}$$

$$1/Y_r = Z_r = Z_{04} = \sqrt{Z_4/Y_4} = \sqrt{\omega\mu_0/\left(\omega\varepsilon_4 + i\sigma_4\right)} H_0^{(1)}\left(k_4 a\right) / \left[2\pi k_4 a H_1^{(1)}\left(k_4 a\right)\right] \tag{126}$$

7.3 Disc Base Plate Termination

For a quasi-static elliptical disc base plate termination, when the ground conductivity is low, we write

$$Z_t^{GP} \to Z_t^{GP} + Z_d = Z_t^{GP} + 1/Y_d$$

With semi-axes $a_d > b_d$, the admittance to infinity in the half space is [16]

$$Y_d = 2\pi a_d \left(\sigma_4 - i\omega\varepsilon_4\right) / K\left(\nu\right) \tag{127}$$

where

$$\nu = \sqrt{1 - b_d^2/a_d^2} \tag{128}$$

and the complete elliptic integral of the first kind is

$$K\left(\nu\right) = \int_0^{\pi/2} d\theta / \sqrt{1 - \nu^2 \sin^2\theta} \tag{129}$$

For a quasi-static circular disc base plate termination of radius $a_d = b_d$ with $K\left(0\right) = \pi/2$ the admittance to infinity in the half space is [16]

$$Y_d = 4a_d\left(\sigma_4 - i\omega\varepsilon_4\right) \tag{130}$$

Note that using $K\left(\nu\right) \sim \ln\left(4/\sqrt{1-\nu^2}\right)$, $\nu \to 1$ we find

$$Y_d \sim 2\pi a_d \left(\sigma_4 - i\omega\varepsilon_4\right) / \ln\left(4a_d/b_d\right) \ , \ b_d << a_d \tag{131}$$

8 DIELECTRIC COATING

Now if there is a thin layer of radius b surrounding the wire, for which the medium is ε_w, the effect can be included by modifying the capacitance per unit length of the transmission line [8], [12]

$$1/C_e \approx \frac{\text{Arccosh}\left(h/b\right)}{\pi\varepsilon'} + \frac{\ln\left(b/a\right)}{\pi\varepsilon_w} \approx \frac{\ln\left(2h/b\right)}{\pi\varepsilon'} + \frac{\ln\left(b/a\right)}{\pi\varepsilon_w} \tag{132}$$

To include the air losses we use the admittance per unit length by

$$1/Y_e = \frac{\text{Arccosh}\left(h/b\right)}{-i\omega\pi\varepsilon} + \frac{\ln\left(b/a\right)}{-i\omega\pi\varepsilon_w} \approx \frac{\ln\left(2h/b\right)}{-i\omega\pi\varepsilon} + \frac{\ln\left(b/a\right)}{-i\omega\pi\varepsilon_w} \tag{133}$$

We ignore this coating at the "shorted" end since the voltage and electric field are small in this region. At the "open" circuit end the electric field is large and we modify the terminating capacitance to

$$C_t \sim C\frac{2h}{\Omega'}\left[1+4\left(1-\ln 2\right)/\Omega'\right] \tag{134}$$

$$\Omega' = 2\left[\ln\left(2h/b\right)+\frac{\varepsilon'}{\varepsilon_w}\ln\left(b/a\right)\right] \tag{135}$$

or in terms of the admittance

$$Y_t \sim Y_e\frac{2h}{\Omega'}\left[1+4\left(1-\ln 2\right)/\Omega'\right] \tag{136}$$

9 RADIATION LOSSES

We first restrict attention to simple open and short end conditions with a high conductivity ground and negligible plasma conduction losses in the air. Later we mention the reflection method which can be used to generalize these results to longer lines and to large skin depths.

The radiation losses are estimated by first finding the magnetic vector potential from the current distribution [17]

$$\underline{A}\left(\underline{r}\right) = \mu_0\int_V \underline{J}\left(\underline{r}'\right)\frac{e^{ik|\underline{r}-\underline{r}'|}}{4\pi\left|\underline{r}-\underline{r}'\right|}dV' \tag{137}$$

Here we neglect the small loss part of the air permittivity and take

$$k \approx \omega\sqrt{\mu_0\varepsilon'} \tag{138}$$

We note that collision losses are included in the transmission line admittance per unit length (as well as the "open" terminating admittance) in ε''. If the imaginary part of the permittivity becomes sizable compared to the real part we would expect the collisional losses to dominate over the radiation. On the other hand, if collisional losses and radiation losses are both small perturbational effects, we would expect that the two loss contributions can be added separately.

Thus there are in general two components of the vector potential

$$A_z\left(x,y,z\right) = \frac{\mu_0}{4\pi}\int_0^\ell I\left(z'\right)\left[\frac{e^{ik\sqrt{(x-h_e)^2+y^2+(z-z')^2}}}{\sqrt{\left(x-h/2\right)^2+y^2+\left(z-z'\right)^2}}-\frac{e^{ik\sqrt{(x+h_e)^2+y^2+(z-z')^2}}}{\sqrt{\left(x+h/2\right)^2+y^2+\left(z-z'\right)^2}}\right]dz' \tag{139}$$

$$A_x\left(x,y,z\right) = \frac{\mu_0}{4\pi}I\left(0\right)\int_{-h_e}^{h_e}\frac{e^{ik\sqrt{(x-x')^2+y^2+z^2}}}{\sqrt{\left(x-x'\right)^2+y^2+z^2}}dx' - \frac{\mu_0}{4\pi}I\left(\ell\right)\int_{-h_e}^{h_e}\frac{e^{ik\sqrt{(x-x')^2+y^2+(z-\ell)^2}}}{\sqrt{\left(x-x'\right)^2+y^2+\left(z-\ell\right)^2}}dx' \tag{140}$$

where we have approximated the currents at the ends as constant and taken the load current $I\left(0\right)$ to be x directed and $I\left(\ell\right)$ to be $-x$ directed.

The far zone fields are found from

$$\underline{H} = \frac{1}{\mu_0}\nabla \times \underline{A} \sim i\frac{k}{\mu_0}\underline{e}_r \times \underline{A} \tag{141}$$

$$\underline{E} = \frac{i}{\omega\varepsilon}\nabla \times \underline{H} \sim -\frac{k}{\omega\varepsilon}\underline{e}_r \times \underline{H} \sim -i\omega\underline{e}_r \times \underline{e}_r \times \underline{A} = i\omega\underline{A}_t \tag{142}$$

where $\underline{A}_t$ denotes transverse to $\underline{r}$ components. The Poynting vector is

$$\underline{S} = \frac{1}{2}\underline{E} \times \underline{H}^* \tag{143}$$

and in the far zone

$$S_r \sim \frac{1}{2\mu_0}\omega k\underline{e}_r \cdot [\underline{A}_t \times (\underline{e}_r \times \underline{A}_t^*)] = \frac{1}{2\mu_0}\omega k \left|\underline{A}_t\right|^2 = \frac{1}{2\mu_0}\omega k\left(|A_\theta|^2 + |A_\varphi|^2\right) \tag{144}$$

where we use the unit vector relations

$$\underline{e}_z = \underline{e}_r \cos\theta - \underline{e}_\theta \sin\theta \tag{145}$$

$$\underline{e}_x = \underline{e}_r \sin\theta\cos\varphi + \underline{e}_\theta \cos\theta\cos\varphi - \underline{e}_\varphi \sin\varphi \tag{146}$$

to convert from Cartesian coordinates. The power radiated is then found by integration over the sphere at infinity

$$P = \int_0^{2\pi}\int_0^{\pi} S_r r^2 \sin\theta d\theta d\varphi$$

$$= \frac{1}{2\mu_0}\omega k\int_0^{2\pi}\int_0^{\pi} |A_\theta|^2 r^2 \sin\theta d\theta d\varphi + \frac{1}{2\mu_0}\omega k\int_0^{2\pi}\int_0^{\pi} |A_\varphi|^2 r^2 \sin\theta d\theta d\varphi \tag{147}$$

9.1 Open-Open Case

Now we will approximate the current distribution along the transmission line to be the half wave form for open circuits

$$I(z) \approx I_0 \sin(k_n z) = I_0 \sin\left(\frac{\pi n z}{\ell}\right)\ ,\ n = 1, 2, 3, ... \tag{148}$$

We are interested in the far zone field

$$\sqrt{(x \mp h_e)^2 + y^2 + (z - z')^2} \sim r \mp h_e \sin\theta\cos\varphi - z'\cos\theta \tag{149}$$

and thus we approximate the potential as

$$A_z \sim \frac{\mu_0}{4\pi r} I_0 \int_0^{\ell} \sin(k_n z') \left[e^{ik\left(r - h_e \sin\theta\cos\varphi - z'\cos\theta\right)} - e^{ik\left(r + h_e \sin\theta\cos\varphi - z'\cos\theta\right)}\right] dz'$$

$$\sim -i\frac{\mu_0 e^{ikr}}{2\pi r} I_0 \sin(kh_e \sin\theta\cos\varphi) \int_0^{\ell} \sin(k_n z')\, e^{-ikz'\cos\theta} dz'$$

$$\sim -\frac{\mu_0 e^{ikr}}{4\pi r} I_0 \sin\left(kh_e \sin\theta\cos\varphi\right) \int_0^{\ell} \left[e^{i(k_n - k\cos\theta)z'} - e^{-i(k_n + k\cos\theta)z'}\right] dz'$$

$$\sim i\frac{\mu_0 e^{ikr}}{4\pi r} I_0 \sin\left(kh_e \sin\theta\cos\varphi\right) \left[\frac{e^{i(k_n - k\cos\theta)\ell} - 1}{(k_n - k\cos\theta)} + \frac{e^{-i(k_n + k\cos\theta)\ell} - 1}{(k_n + k\cos\theta)}\right]$$

$$\sim i\frac{\mu_0 e^{ikr}}{4\pi r} I_0 kh_e \sin\theta\cos\varphi \left[\frac{e^{i(k_n - k\cos\theta)\ell} - 1}{(k_n - k\cos\theta)} + \frac{e^{-i(k_n + k\cos\theta)\ell} - 1}{(k_n + k\cos\theta)}\right] \tag{150}$$

The spherical form of the potential (ignoring A_r) is thus

$$A_\theta \sim -i\frac{\mu_0 e^{ikr}}{4\pi r} I_0 kh_e \sin^2\theta\cos\varphi \left[\frac{e^{i(k_n - k\cos\theta)\ell} - 1}{(k_n - k\cos\theta)} + \frac{e^{-i(k_n + k\cos\theta)\ell} - 1}{(k_n + k\cos\theta)}\right] \tag{151}$$

The power radiated is

$$P = \frac{1}{2\mu_0}\omega k \int_0^{2\pi}\int_0^{\pi} \left|A_\theta\right|^2 r^2 \sin\theta d\theta d\varphi$$

$$= \frac{\omega\mu_0}{32\pi^2}\left|I_0\right|^2 k^3 h_e^2 \int_0^{2\pi} \cos^2\varphi d\varphi \int_0^{\pi} \left|\frac{e^{i(k_n - k\cos\theta)\ell} - 1}{(k_n - k\cos\theta)} + \frac{e^{-i(k_n + k\cos\theta)\ell} - 1}{(k_n + k\cos\theta)}\right|^2 \sin^5\theta d\theta$$

$$= \frac{\omega\mu_0}{32\pi}\left|I_0\right|^2 k^3 h_e^2 \int_{-1}^{1} \left|\frac{e^{i(k_n - ku)\ell} - 1}{(k_n - ku)} + \frac{e^{-i(k_n + ku)\ell} - 1}{(k_n + ku)}\right|^2 \left(1 - u^2\right)^2 du \tag{152}$$

Now taking $k_n = \pi n/\ell \to k$

$$P = \frac{\omega\mu_0}{32\pi}\left|I_0\right|^2 kh_e^2 \int_{-1}^{1} \left|(1+u)\left\{e^{ik\ell(1-u)} - 1\right\} + (1-u)\left\{e^{-ik\ell(1+u)} - 1\right\}\right|^2 du$$

$$= \frac{\omega\mu_0}{8\pi}\left|I_0\right|^2 kh_e^2 \int_{-1}^{1} \left|\left\{\cos\left(k\ell\right) + iu\sin\left(k\ell\right)\right\} e^{-ik\ell u} - 1\right|^2 du$$

$$= \frac{\omega\mu_0}{8\pi}\left|I_0\right|^2 kh_e^2 \int_{-1}^{1} \left[\left\{\cos\left(k\ell\right)\cos\left(k\ell u\right) + u\sin\left(k\ell\right)\sin\left(k\ell u\right) - 1\right\}^2 + \left\{u\sin\left(k\ell\right)\cos\left(k\ell u\right) - \cos\left(k\ell\right)\sin\left(k\ell u\right)\right\}^2\right] du$$

$$= \frac{\omega\mu_0}{4\pi}\left|I_0\right|^2 kh_e^2 \int_0^{1} \left[1 + \cos^2\left(k\ell\right) + u^2\sin^2\left(k\ell\right) - 2\cos\left(k\ell\right)\cos\left(k\ell u\right) - 2u\sin\left(k\ell\right)\sin\left(k\ell u\right)\right] du$$

$$= \frac{\omega\mu_0}{4\pi}\left|I_0\right|^2 kh_e^2 \left[1 + \cos^2\left(k\ell\right) + \frac{1}{3}\sin^2\left(k\ell\right) - \frac{2}{\left(k\ell\right)^2}\sin^2\left(k\ell\right)\right]$$

$$= \frac{\omega\mu_0}{2\pi}\left|I_0\right|^2 kh_e^2 \ , \ k\ell \to n\pi \tag{153}$$

where we used

$$\int u \sin(k\ell u)\, du = -\frac{u}{k\ell}\cos(k\ell u) + \frac{1}{(k\ell)^2}\sin(k\ell u) \tag{154}$$

Suppose we set this equal to

$$P = \frac{1}{2}G_{rad}\left|V(0)\right|^2 + \frac{1}{2}G_{rad}\left|V(\ell)\right|^2 \tag{155}$$

where

$$\frac{dI}{dz} = i\omega CV \approx k_n I_0 \cos(k_n z) = k_n I_0 \cos\left(\frac{\pi n z}{\ell}\right) \tag{156}$$

and thus

$$V(0) = \frac{k_n}{i\omega C} I_0 = -iZ_c I_0 \tag{157}$$

$$V(\ell) = \frac{k_n}{i\omega C} I_0 (-1)^n = -iZ_c I_0 (-1)^n \tag{158}$$

or

$$P = Z_c^2 G_{rad}\left|I_0\right|^2 \tag{159}$$

Then we find

$$G_{rad} = \frac{\omega\mu_0}{2\pi Z_c^2} k h_e^2 = \frac{\pi (k h_e)^2/\eta}{2\ln^2(2h_e/a)} \ , \ k\ell \to n\pi \tag{160}$$

using the characteristic impedance

$$Z_c = \frac{\eta}{\pi}\ln(2h_e/a) \ , \ \eta = \sqrt{\mu_0/\varepsilon'} \tag{161}$$

With the ground plane we find half this result (for radiation only into the upper half space)

$$G_{rad}^{GP} = \frac{\omega\mu_0}{4\pi Z_c^{GP2}} k h_e^2 = \frac{\pi (k h_e)^2/\eta}{\ln^2(2h_e/a)} \ , \ k\ell \to n\pi \tag{162}$$

where the characteristic impedance is also cut in half (since the voltage is only the contribution above the ground plane)

$$Z_c^{GP} = \frac{\eta}{2\pi}\ln(2h_e/a) \tag{163}$$

9.2 Short-Short Case

Now we will approximate the current distribution along the transmission line to be the half wave form for short circuits

$$I(z) \approx I(0)\cos(k_n z) = I(0)\cos\left(\frac{\pi n z}{\ell}\right)\ ,\ n = 1,2,3,... \tag{164}$$

Using the far zone approximations

$$\sqrt{(x-x')^2+y^2+z^2} \sim r - x'\sin\theta\cos\varphi \tag{165}$$

$$\sqrt{(x-x')^2+y^2+(z-\ell)^2} \sim r - x'\sin\theta\cos\varphi - \ell\cos\theta \tag{166}$$

we find

$$\begin{aligned}
A_z &\sim \frac{\mu_0}{4\pi r} I(0) \int_0^\ell \cos(k_n z') \left[e^{ik\left(r - h_e \sin\theta\cos\varphi - z'\cos\theta\right)} - e^{ik\left(r + h_e \sin\theta\cos\varphi - z'\cos\theta\right)} \right] dz' \\
&\sim -i\frac{\mu_0 e^{ikr}}{4\pi r} I(0)\sin(k h_e \sin\theta\cos\varphi) \int_0^\ell \left[e^{i(k_n - k\cos\theta)z'} + e^{-i(k_n + k\cos\theta)z'} \right] dz' \\
&\sim -\frac{\mu_0 e^{ikr}}{4\pi r} I(0)\sin(k h_e \sin\theta\cos\varphi) \left[\frac{e^{i(k_n - k\cos\theta)\ell} - 1}{(k_n - k\cos\theta)} - \frac{e^{-i(k_n + k\cos\theta)\ell} - 1}{(k_n + k\cos\theta)} \right] \\
&\sim -\frac{\mu_0 e^{ikr}}{4\pi r} I(0)\, k h_e \sin\theta\cos\varphi \left[\frac{e^{i(k_n - k\cos\theta)\ell} - 1}{(k_n - k\cos\theta)} - \frac{e^{-i(k_n + k\cos\theta)\ell} - 1}{(k_n + k\cos\theta)} \right]
\end{aligned} \tag{167}$$

$$\begin{aligned}
A_x &\sim \frac{\mu_0}{4\pi r} I(0) \int_{-h_e}^{h_e} e^{ik\left(r - x'\sin\theta\cos\varphi\right)} dx' - \frac{\mu_0}{4\pi r} I(\ell) \int_{-h_e}^{h_e} e^{ik\left(r - x'\sin\theta\cos\varphi - \ell\cos\theta\right)} dx' \\
&\sim \frac{\mu_0 e^{ikr}}{2\pi kr} \left[I(0) - I(\ell)\, e^{-ik\ell\cos\theta} \right] \frac{\sin(k h_e \sin\theta\cos\varphi)}{\sin\theta\cos\varphi} \\
&\sim \frac{\mu_0 e^{ikr - ik(\ell/2)\cos\theta}}{2\pi kr} I(0) \left[e^{ik(\ell/2)\cos\theta} - (-1)^n\, e^{-ik(\ell/2)\cos\theta} \right] \frac{\sin(k h_e \sin\theta\cos\varphi)}{\sin\theta\cos\varphi} \\
&\sim \left\{ \begin{array}{c} i \\ 1 \end{array} \right\} \frac{\mu_0 e^{ikr - ik(\ell/2)\cos\theta}}{\pi kr \sin\theta\cos\varphi} I(0) \left\{ \begin{array}{c} \sin[k(\ell/2)\cos\theta] \\ \cos[k(\ell/2)\cos\theta] \end{array} \right\} \sin[k h_e \sin\theta\cos\varphi]\ ,\ \left\{ \begin{array}{c} n \text{ even} \\ n \text{ odd} \end{array} \right\} \\
&\sim \left\{ \begin{array}{c} i \\ 1 \end{array} \right\} \frac{\mu_0 e^{ikr - ik(\ell/2)\cos\theta}}{\pi r} I(0)\, h_e \left\{ \begin{array}{c} \sin[k(\ell/2)\cos\theta] \\ \cos[k(\ell/2)\cos\theta] \end{array} \right\}\ ,\ \left\{ \begin{array}{c} n \text{ even} \\ n \text{ odd} \end{array} \right\}
\end{aligned} \tag{168}$$

The spherical form of the potential (ignoring A_r) is then

$$A_\theta \sim \frac{\mu_0 e^{ikr}}{\pi r} I(0)\, h_e \cos\varphi$$

$$\left[\frac{1}{4} k \sin^2\theta \left\{ \frac{e^{i(k_n - k\cos\theta)\ell} - 1}{(k_n - k\cos\theta)} - \frac{e^{-i(k_n + k\cos\theta)\ell} - 1}{(k_n + k\cos\theta)} \right\} + \left\{ \begin{array}{c} i \\ 1 \end{array} \right\} e^{-ik(\ell/2)\cos\theta} \left\{ \begin{array}{c} \sin(k(\ell/2)\cos\theta) \\ \cos(k(\ell/2)\cos\theta) \end{array} \right\} \cos\theta \right]$$

$$\sim i\frac{\mu_0 e^{ikr-ik(\ell/2)\cos\theta}}{\pi r}I\left(0\right)h_e\cos\varphi$$

$$\left[\frac{1}{2}k\sin^2\theta\left\{e^{ik_n\ell/2}\frac{\sin\left(\left(k_n-k\cos\theta\right)\ell/2\right)}{\left(k_n-k\cos\theta\right)}+e^{-ik_n\ell/2}\frac{\sin\left(\left(k_n+k\cos\theta\right)\ell/2\right)}{\left(k_n+k\cos\theta\right)}\right\}+\left\{\begin{array}{c}1\\-i\end{array}\right\}\left\{\begin{array}{c}\sin\left(k\left(\ell/2\right)\cos\theta\right)\\\cos\left(k\left(\ell/2\right)\cos\theta\right)\end{array}\right\}\cos\theta\right] \tag{169}$$

$$A_\varphi\sim-\left\{\begin{array}{c}i\\1\end{array}\right\}\frac{\mu_0 e^{ikr-ik(\ell/2)\cos\theta}}{\pi r}I\left(0\right)h_e\sin\varphi\left\{\begin{array}{c}\sin\left(k\left(\ell/2\right)\cos\theta\right)\\\cos\left(k\left(\ell/2\right)\cos\theta\right)\end{array}\right\},\left\{\begin{array}{c}n\text{ even}\\n\text{ odd}\end{array}\right\} \tag{170}$$

The power radiated is then

$$P=\frac{1}{2\mu_0}\omega k\int_0^{2\pi}\int_0^{\pi}\left|A_\theta\right|^2 r^2\sin\theta d\theta d\varphi+\frac{1}{2\mu_0}\omega k\int_0^{2\pi}\int_0^{\pi}\left|A_\varphi\right|^2 r^2\sin\theta d\theta d\varphi \tag{171}$$

or

$$P/\left[\frac{\mu_0 h_e^2}{2\pi}\omega k\left|I\left(0\right)\right|^2\right]$$

$$=\int_0^{\pi}\left|\frac{1}{2}k\sin^2\theta\left\{e^{ik_n\ell/2}\frac{\sin\left(\left(k_n-k\cos\theta\right)\ell/2\right)}{\left(k_n-k\cos\theta\right)}+e^{-ik_n\ell/2}\frac{\sin\left(\left(k_n+k\cos\theta\right)\ell/2\right)}{\left(k_n+k\cos\theta\right)}\right\}\right.$$

$$\left.+\left\{\begin{array}{c}1\\-i\end{array}\right\}\left\{\begin{array}{c}\sin\left(k\left(\ell/2\right)\cos\theta\right)\\\cos\left(k\left(\ell/2\right)\cos\theta\right)\end{array}\right\}\cos\theta\right|^2\sin\theta d\theta+\int_0^{\pi}\left\{\begin{array}{c}\sin^2\left(k\left(\ell/2\right)\cos\theta\right)\\\cos^2\left(k\left(\ell/2\right)\cos\theta\right)\end{array}\right\}\sin\theta d\theta$$

$$=\int_{-1}^{1}\left|\frac{1}{2}k\left(1-u^2\right)\left\{e^{ik_n\ell/2}\frac{\sin\left(\left(k_n-ku\right)\ell/2\right)}{\left(k_n-ku\right)}+e^{-ik_n\ell/2}\frac{\sin\left(\left(k_n+ku\right)\ell/2\right)}{\left(k_n+ku\right)}\right\}+\left\{\begin{array}{c}1\\-i\end{array}\right\}\left\{\begin{array}{c}\sin\left(k\left(\ell/2\right)u\right)\\\cos\left(k\left(\ell/2\right)u\right)\end{array}\right\}u\right|^2 du$$

$$+\int_{-1}^{1}\left\{\begin{array}{c}\sin^2\left(k\left(\ell/2\right)u\right)\\\cos^2\left(k\left(\ell/2\right)u\right)\end{array}\right\}du \tag{172}$$

Now taking $k_n=n\pi/\ell\to k$

$$P/\left[\frac{\mu_0 h_e^2}{2\pi}\omega k\left|I\left(0\right)\right|^2\right]$$

$$=\int_{-1}^{1}\left|\frac{1}{2}\left\{e^{ik_n\ell/2}\left(1+u\right)\sin\left(\left(1-u\right)k\ell/2\right)+e^{-ik_n\ell/2}\left(1-u\right)\sin\left(\left(1+u\right)k\ell/2\right)\right\}+\left\{\begin{array}{c}1\\-i\end{array}\right\}\left\{\begin{array}{c}\sin\left(k\left(\ell/2\right)u\right)\\\cos\left(k\left(\ell/2\right)u\right)\end{array}\right\}u\right|^2 du$$

$$+\int_{-1}^{1}\left\{\begin{array}{c}\sin^2\left(k\left(\ell/2\right)u\right)\\\cos^2\left(k\left(\ell/2\right)u\right)\end{array}\right\}du=\int_{-1}^{1}\left|\frac{1}{2}\sin\left(k\ell\right)\cos\left(k\ell u/2\right)-u\cos^2\left(k\ell/2\right)\sin\left(k\ell u/2\right)\right.$$

$$\left.-i\frac{1}{2}\sin\left(k\ell\right)\sin\left(k\ell u/2\right)+iu\sin^2\left(k\ell/2\right)\cos\left(k\ell u/2\right)+\left\{\begin{array}{c}1\\-i\end{array}\right\}\left\{\begin{array}{c}\sin\left(k\left(\ell/2\right)u\right)\\\cos\left(k\left(\ell/2\right)u\right)\end{array}\right\}u\right|^2 du$$

$$+\int_{-1}^{1}\left\{\begin{array}{c}\sin^2\left(k\left(\ell/2\right)u\right)\\\cos^2\left(k\left(\ell/2\right)u\right)\end{array}\right\}du$$

$$= \frac{1}{2}\int_0^1 \left[\sin^2(k\ell) + 4u^2 \left\{ \begin{array}{c} \sin^4(k\ell/2) \\ \cos^4(k\ell/2) \end{array} \right\}\right] du + \int_0^1 \{1 \mp \cos(k\ell u)\}\, du$$

$$= \frac{1}{2}\left[\sin^2(k\ell) + \frac{4}{3}\left\{ \begin{array}{c} \sin^4(k\ell/2) \\ \cos^4(k\ell/2) \end{array} \right\}\right] + \left\{1 \mp \frac{\sin(k\ell)}{k\ell}\right\} \tag{173}$$

Thus

$$P/\left[\frac{\mu_0 h_e^2}{2\pi}\omega k \left|I(0)\right|^2\right] = 1\ , k\ell \to n\pi\ \ , \ \left\{ \begin{array}{c} n \text{ even} \\ n \text{ odd} \end{array} \right\} \tag{174}$$

Now setting

$$P = \frac{1}{2}R_{rad}\left|I(0)\right|^2 + \frac{1}{2}R_{rad}\left|I(\ell)\right|^2 = R_{rad}\left|I(0)\right|^2 \tag{175}$$

we find

$$R_{rad} = \frac{\eta}{2\pi}(kh_e)^2\ \ , \ k\ell \to n\pi \tag{176}$$

or for the half space

$$R_{rad}^{GP} = \frac{\eta(kh_e)^2}{4\pi}\ , \ k\ell \to n\pi \tag{177}$$

9.3 Open-Short Case

Now we will approximate the current distribution along the transmission line to be

$$I(z) \approx I(\ell)(-1)^{(n-1)/2}\sin(k_n z) = I(\ell)(-1)^{(n-1)/2}\sin\left(\frac{\pi n z'}{2\ell}\right)\ , \ n = 1, 3, 5, ... \tag{178}$$

We are interested in the far zone field

$$A_z \sim \frac{\mu_0}{4\pi r} I(\ell)(-1)^{(n-1)/2}\int_0^\ell \sin(k_n z')\left[e^{ik\left(r - h_e\sin\theta\cos\varphi - z'\cos\theta\right)} - e^{ik\left(r + h_e\sin\theta\cos\varphi - z'\cos\theta\right)}\right] dz'$$

$$\sim -i\frac{\mu_0 e^{ikr}}{2\pi r} I(\ell)(-1)^{(n-1)/2}\sin\{kh_e\sin\theta\cos\varphi\}\int_0^\ell \sin(k_n z')\, e^{-ikz'\cos\theta} dz'$$

$$\sim -\frac{\mu_0 e^{ikr}}{4\pi r} I(\ell)(-1)^{(n-1)/2}\sin\{kh_e\sin\theta\cos\varphi\}\int_0^\ell \left[e^{i(k_n - k\cos\theta)z'} - e^{-i(k_n + k\cos\theta)z'}\right] dz'$$

$$\sim i\frac{\mu_0 e^{ikr}}{4\pi r} I(\ell)(-1)^{(n-1)/2}\sin\{kh_e\sin\theta\cos\varphi\}\left[\frac{e^{i(k_n - k\cos\theta)\ell} - 1}{(k_n - k\cos\theta)} + \frac{e^{-i(k_n + k\cos\theta)\ell} - 1}{(k_n + k\cos\theta)}\right] \tag{179}$$

Now taking $k_n = n\pi/(2\ell) \to k$

$$A_z \sim i\frac{\mu_0 e^{ikr}}{4\pi r} I(\ell)(-1)^{(n-1)/2} h_e \sin\theta\cos\varphi \left[\frac{e^{ik\ell(1-\cos\theta)}-1}{(1-\cos\theta)} + \frac{e^{-ik\ell(1+\cos\theta)}-1}{(1+\cos\theta)}\right] \tag{180}$$

Similarly

$$A_x \sim -\frac{\mu_0}{4\pi r} I(\ell) \int_{-h_e}^{h_e} e^{ik\left(r - x'\sin\theta\cos\varphi - \ell\cos\theta\right)} dx'$$

$$\sim -\frac{\mu_0 e^{ik(r-\ell\cos\theta)}}{4\pi r} I(\ell) \int_{-h_e}^{h_e} e^{-ikx'\sin\theta\cos\varphi} dx'$$

$$\sim -\frac{\mu_0 e^{ik(r-\ell\cos\theta)}}{2\pi r} I(\ell) \frac{\sin\{kh_e\sin\theta\cos\varphi\}}{k\sin\theta\cos\varphi} \sim -\frac{\mu_0 e^{ik(r-\ell\cos\theta)}}{2\pi r} I(\ell) h_e \tag{181}$$

where we have assumed that $kh_e << 1$ and the final form is that associated with a small dipole. The far field spherical form of the potential (ignoring A_r) is

$$A_\theta \sim -\frac{\mu_0 e^{ik(r-\ell\cos\theta)}}{2\pi r} I(\ell) h_e \cos\theta\cos\varphi$$

$$-i\frac{\mu_0 e^{ikr}}{4\pi r} I(\ell)(-1)^{(n-1)/2} h_e \sin^2\theta\cos\varphi \left\{\frac{e^{ik\ell(1-\cos\theta)}-1}{(1-\cos\theta)} + \frac{e^{-ik\ell(1+\cos\theta)}-1}{(1+\cos\theta)}\right\}$$

$$\sim -\frac{\mu_0 e^{ik(r-\ell\cos\theta)}}{2\pi r} I(\ell) h_e \cos\theta\cos\varphi$$

$$-i\frac{\mu_0 e^{ikr}}{4\pi r} I(\ell)(-1)^{(n-1)/2} h_e \cos\varphi \left\{e^{ik\ell(1-\cos\theta)}(1+\cos\theta) + e^{-ik\ell(1+\cos\theta)}(1-\cos\theta) - 2\right\}$$

$$\sim -\frac{\mu_0 e^{ik(r-\ell\cos\theta)}}{2\pi r} I(\ell) h_e \cos\theta\cos\varphi - i\frac{\mu_0 e^{ik(r-\ell\cos\theta)}}{2\pi r} I(\ell)(-1)^{(n-1)/2} h_e \cos\varphi \left\{\cos(k\ell) + i\sin(k\ell)\cos\theta - e^{ik\ell\cos\theta}\right\}$$

$$\sim \frac{e^{ik(r-\ell\cos\theta)}}{2\pi r} h_e \mu_0 I(\ell) \left[\left\{-1 + (-1)^{(n-1)/2}\sin(k\ell)\right\}\cos\theta - i(-1)^{(n-1)/2}\cos(k\ell) + i(-1)^{(n-1)/2} e^{ik\ell\cos\theta}\right]\cos\varphi \tag{182}$$

$$A_\varphi \sim \frac{\mu_0 e^{ik(r-\ell\cos\theta)}}{2\pi r} I(\ell) h_e \sin\varphi \tag{183}$$

The power radiated is now found by integrating over the sphere at infinity

$$P = \frac{1}{2\mu_0}\omega k \int_0^{2\pi}\int_0^{\pi} |A_\theta|^2 r^2 \sin\theta d\theta d\varphi + \frac{1}{2\mu_0}\omega k \int_0^{2\pi}\int_0^{\pi} |A_\varphi|^2 r^2 \sin\theta d\theta d\varphi$$

$$= \frac{1}{8\pi}\omega\mu_0 k \left|I\left(\ell\right)\right|^2 h_e^2 \int_{-1}^{1} \left|\left\{-1+\left(-1\right)^{(n-1)/2}\sin\left(k\ell\right)\right\}u - i\left(-1\right)^{(n-1)/2}\cos\left(k\ell\right) + i\left(-1\right)^{(n-1)/2} e^{ik\ell u}\right|^2 du$$

$$+\frac{1}{8\pi}\omega\mu_0 k \left|I\left(\ell\right)\right|^2 h_e^2 \int_{-1}^{1} du$$

$$= \frac{1}{8\pi}\omega\mu_0 k \left|I\left(\ell\right)\right|^2 h_e^2 \int_{-1}^{1} \left|\left\{\left(-1\right)^{(n+1)/2}+\sin\left(k\ell\right)\right\}u - i\cos\left(k\ell\right) + ie^{ik\ell u}\right|^2 du$$

$$+\frac{1}{4\pi}\omega\mu_0 k \left|I\left(\ell\right)\right|^2 h_e^2$$

$$= \frac{1}{8\pi}\omega\mu_0 k \left|I\left(\ell\right)\right|^2 h_e^2 \int_{-1}^{1} \left|\left\{\left(-1\right)^{(n+1)/2}+\sin\left(k\ell\right)\right\}u - \sin\left(k\ell u\right) - i\cos\left(k\ell\right) + i\cos\left(k\ell u\right)\right|^2 du$$

$$+\frac{1}{4\pi}\omega\mu_0 k \left|I\left(\ell\right)\right|^2 h_e^2$$

$$= \frac{1}{8\pi}\omega\mu_0 k \left|I\left(\ell\right)\right|^2 h_e^2$$

$$\int_{-1}^{1}\left[\left\{\left(-1\right)^{(n+1)/2}+\sin\left(k\ell\right)\right\}^2 u^2 - 2\left\{\left(-1\right)^{(n+1)/2}+\sin\left(k\ell\right)\right\}u\sin\left(k\ell u\right) + 1 + \cos^2\left(k\ell\right) - 2\cos\left(k\ell u\right)\cos\left(k\ell\right)\right] du$$

$$+\frac{1}{4\pi}\omega\mu_0 k \left|I\left(\ell\right)\right|^2 h_e^2$$

$$= \frac{1}{4\pi}\omega\mu_0 k \left|I\left(\ell\right)\right|^2 h_e^2 \left[1+\frac{1}{3}\left\{\left(-1\right)^{(n+1)/2}+\sin\left(k\ell\right)\right\}^2\right.$$

$$\left.-2\left\{\left(-1\right)^{(n+1)/2}+\sin\left(k\ell\right)\right\}\left\{-\frac{1}{k\ell}\cos\left(k\ell\right)+\frac{1}{k^2\ell^2}\sin\left(k\ell\right)\right\}+1+\cos^2\left(k\ell\right)-\frac{2}{k\ell}\sin\left(k\ell\right)\cos\left(k\ell\right)\right] \quad (184)$$

Letting $k\ell = n\pi/2\ ,\ n = 1,3,5,...$

$$P = \frac{1}{2\pi}\omega\mu_0 k \left|I\left(\ell\right)\right|^2 h_e^2 \quad (185)$$

If we take

$$P = \frac{1}{2}G_{rad}\left|V\left(0\right)\right|^2 + \frac{1}{2}R_{rad}\left|I\left(\ell\right)\right|^2 \quad (186)$$

$$\frac{dI}{dz} = i\omega CV = k_n I\left(\ell\right)\cos\left(k_n z\right) \quad (187)$$

$$V(0) = \frac{k_n}{i\omega C} I(\ell) = -iZ_c I(\ell) \tag{188}$$

$$G_{rad} Z_c^2 + R_{rad} = \frac{\eta}{\pi} (kh_e)^2 \tag{189}$$

We could place this perturbing radiation term exclusively at the shorted end, or exclusively at the open end, by setting the other term to zero. Note from the open-open and the short-short cases above we had

$$G_{rad} Z_c^2 = \eta (kh_e)^2 / (2\pi) = R_{rad} \tag{190}$$

which adds up to this same result, and hence it is better to add these radiation loads on each end of the open-short setup. One half these values correspond to the ground plane case

$$G_{rad}^{GP} Z_c^{GP2} = \eta (kh_e)^2 / (4\pi) = R_{rad}^{GP} \tag{191}$$

$$G_{rad}^{GP} Z_c^{GP2} + R_{rad}^{GP} = \frac{\eta}{2\pi} (kh_e)^2 \tag{192}$$

9.4 End Reflection Method

To treat radiation from longer lines ending in open circuits, particularly with large skin depths, it is more convenient to change to the description of a reflection from the line end by means of the Wiener-Hopf method as was done for the long antenna [19]. This has been examined both for the semi-infinite wire above a perfectly conducting ground [20], [21], [22], which yields the same radiation result (changing from R_{rad} to G_{rad} for $kh << 1$) as obtained above in the open-open case (162). The semi-infinite and finite wire above a finite conductivity ground has also been treated [23], [24].

10 COMPARISON OF CST SIMULATIONS WITH ATLOG INCLUDING RADIATION

We now compare simulations of transmission lines with various terminations when both terminating reactive loads in addition to radiation resistive loads are included. Again, full wave simulations of transmission lines above a perfectly conducting ground using CST Microwave Studio software, are compared with calculations using the transmission line equations labeled as ATLOG (Analytic Transmission Line Over Ground). All these comparisons are for the case of normal incidence and use a simple unit electric field amplitude sine-squared pulse of 200 ns duration. The line has height $h = 5$ m and a radius of $a = 1$ cm (there is no insulation coating and the wire is a perfect conductor).

Figure 4 shows a comparison of simulations when the ends of a 20 m long section of line are open circuited. The red dashed curve is the full wave simulation, the blue dotted curve is ATLOG with idealized open circuits at the ends, the black solid curve is ATLOG with capacitive loads at the ends, and the green dash-dot curve is ATLOG with capacitive and radiation conductance loads at the ends of the line. Notice that the green dash-dot and red dashed curves are showing reasonable agreement at the later times and are illustrating decay in amplitude due to radiation (there is no other loss in the problem being modeled).

Figure 5 shows a comparison of simulations when the ends of a 20 m long section of line are open circuited on the left and short circuited on the right. The red dashed curve is the full wave simulation,

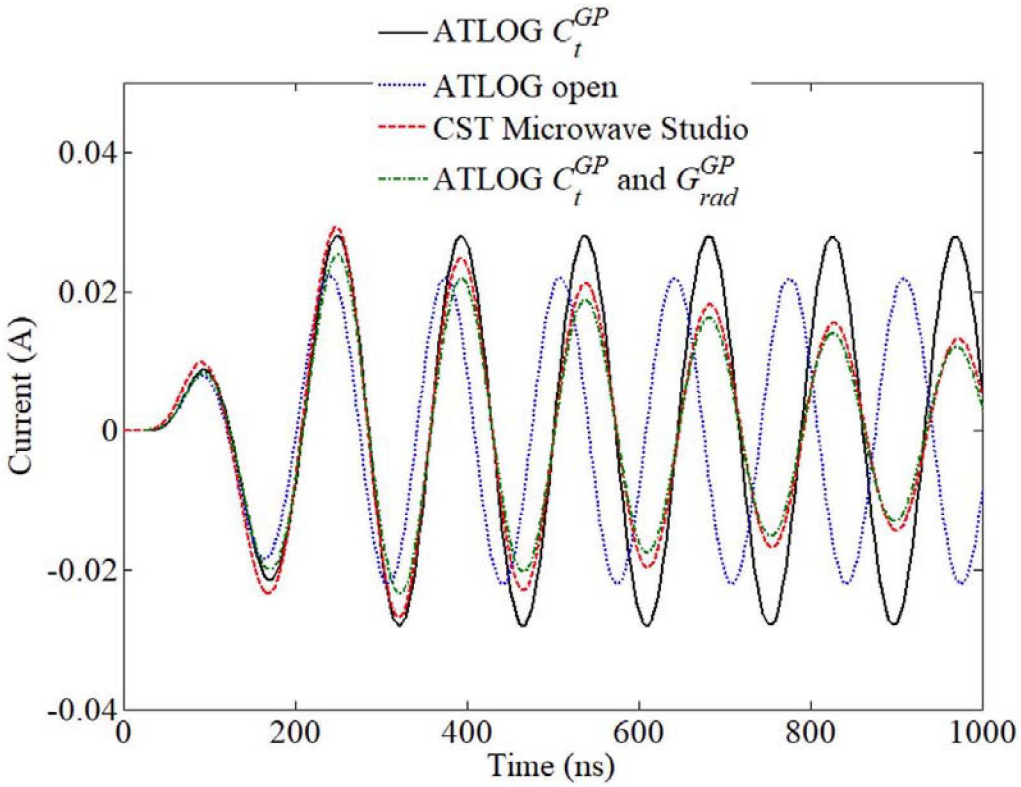

Figure 4. Comparison of full wave simulation (red dashed curve) using CST Microwave Studio with the ATLOG transmission line calculations for a 20 m long section of line having open circuits at both ends. The blue dotted curve has idealized open circuits at each end, the black solid curve has terminating capacitors at each end, and the green dash-dot curve has terminating capacitors and radiation conductances at each end.

the blue dotted curve is ATLOG with idealized open and short circuits at the two ends, the black solid curve is ATLOG with a capacitive load on the left end and an inductive load on the right end, and the green dash-dot curve is ATLOG with capacitive-radiation conductance load on the left end and an inductive-radiation resistance load on the right end. Notice that the blue dotted curve is dominated by a single ringing frequency (phase shifted from the other curves) whereas the black solid curve is exhibiting two ringing frequencies and phase alignment with the red dashed and green dash-dot curves. The radiation damping (proportional to the square of the wavenumber and line height) reduces the amplitude of the higher frequency and results in much better agreement between the ATLOG green dash-dot curve and the full wave simulation.

Figure 6 shows a comparison of simulations when the ends of a 40 m long section of line are short circuited. The red dashed curve is the full wave simulation, the blue dotted curve is ATLOG with idealized short circuits at the ends, the black solid curve is ATLOG with inductive loads at the ends, and the green dash-dot curve is ATLOG with inductive and radiation resistance loads at the ends of the line. Notice that the green dash-dot and red dashed curves are showing reasonable agreement at later times and are illustrating decay in amplitude due to radiation (there is no other loss in the problem being modeled).

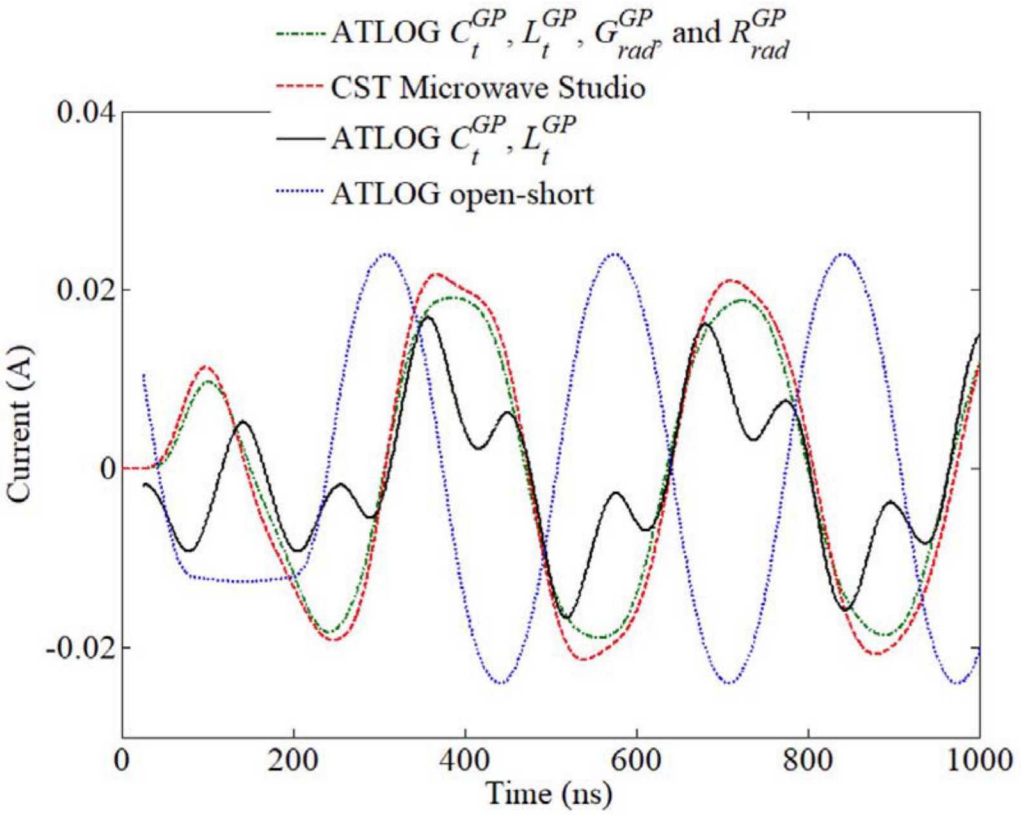

Figure 5. Comparison of full wave simulation (red dashed curve) using CST Microwave Studio with the ATLOG transmission line calculations for a 20 m long section of line having an open circuit at the left end and a short circuit at the right end. The blue dotted curve has idealized open and short circuits at the two ends, the black solid curve has a terminating capacitor and inductor at the respective ends, and the green dash-dot curve has terminating capacitor-radiation conductance and inductor-radiation resistance at the respective ends.

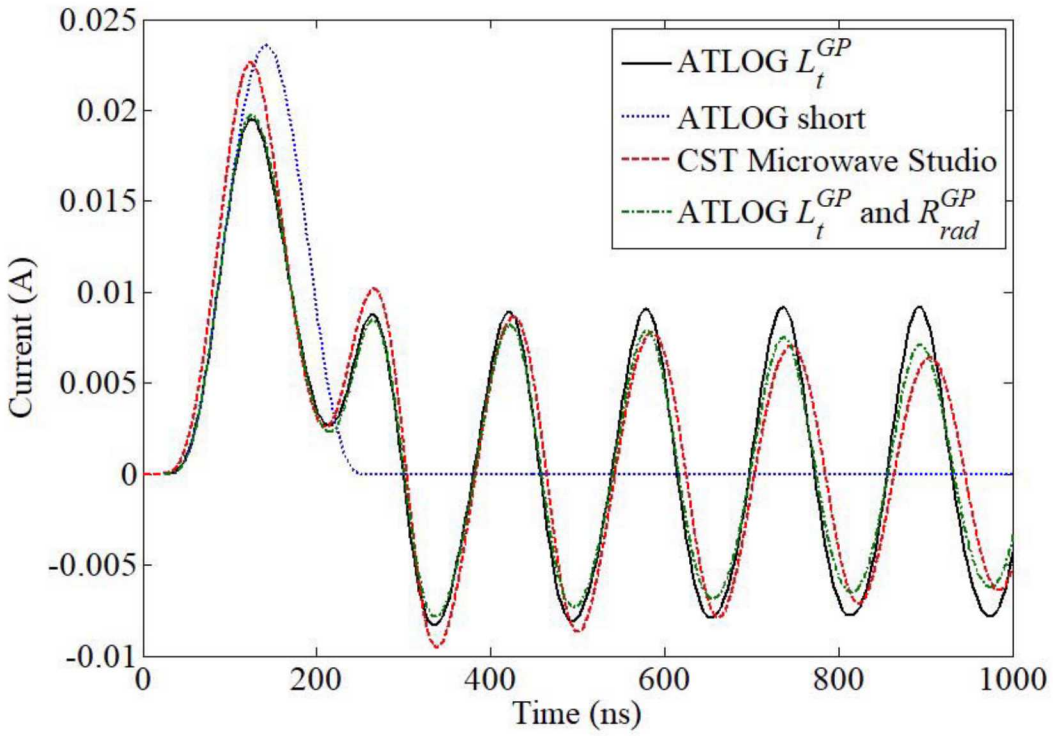

Figure 6. Comparison of full wave simulation (red dashed curve) using CST Microwave Studio with the ATLOG transmission line calculations for a 40 m long section of line having short circuits at both ends. The blue dotted curve has idealized short circuits at each end (and has no ringing at normal incidence), the black solid curve has terminating inductors at each end and shows ringing, and the green dash-dot curve has terminating inductors and radiation resistances at each end.

11 CONCLUSIONS

This report constructs circuit models for the end loads used in a transmission line model of a wire above the earth driven by an electromagnetic field. The cases where the ends of the line are left open, as well as the case where they are connected to the ground, are both treated. In the open case the effective capacitance (and conductance if the air is lossy) is estimated to represent the charge build up near the end of the line. In the shorted case the inductance, in addition to the ground rod or pad impedance, are both estimated. The radiation damping is also discussed for various types of basic terminations. Good agreement is shown versus full wave simulations of lines with open or short terminations.

To sort out the sources in these transmission line models we also compare two different types of model for the plane coupling to these lines and the corresponding meaning of the voltage and current solutions. Finally, we briefly discuss the decomposition of the currents along the line into antenna and transmission line modes.

12 REFERENCES

[1] S. Ramo, J. R. Whinnery, and T. Van Duzer, **Fields and Waves in Communication Electronics**, New York: John Wiley & Sons, Inc., 1965, Ch. 1, Table 8.09, Section 12.28.

[2] E. F. Vance, **Coupling to shielded cables**. New York (NY): John Wiley and Sons; 1987.

[3] K. S. H. Lee, **EMP interaction principles, techniques, and reference data**. Washington: Hemisphere Publishing Corp.; 1986.

[4] J. R. Carson, "Wave propagation in overhead wires with ground return," Bell Syst. Tech. J. 1926;5:539–554.

[5] E. D. Sunde, **Earth Conduction Effects in Transmission Systems**. New York (NY): Dover; 1967.

[6] J. R. Wait, "Theory of wave propagation along a thin wire parallel to an interface," Radio Sci. 1972;7:675–679.

[7] J. R. Wait, "Tutorial note on the general transmission line theory for a thin wire above the ground," IEEE Trans Electromagn. Compat., 1991;33:65–67.

[8] L. K. Warne and K. C. Chen, "Long Line Coupling Models," SAND2004-0872, March 2004.

[9] S. Campione, L. K. Warne, L. I. Basilio, C. D. Turner, K. L. Cartwright, and K. C. Chen, "Electromagnetic pulse excitation of finite- and infinitely-long lossy conductors over a lossy ground plane," Journal of Electromagnetic Waves and Applications, 2017, DOI: 10.1080/09205071.2016.1270776.

[10] K. S. H. Lee, "Two Parallel Terminated Conductors In External Fields," IEEE Transactions on Electromagnetic Compatibility, Vol. EMC-20, No. 2, May 1978, pp. 288-296.

[11] F. M. Tesche, M. V. Ianoz, T. Karlsson, **EMC Analysis Methods And Computational Models**, Ch. 7.

[12] L. K. Warne, W. A. Johnson, R. S. Coats, R. E. Jorgenson, and G. A. Hebner, "Model For Resonant Plasma Probe," Sandia National Laboratories Report, SAND2007-2513, April 2007.

[13] F. W. Grover, **Inductance Calculations**, New York: Dover Pub., Inc., 1946, p. 60.

[14] S. A. Schelkunoff, **Advanced Antenna Theory**, New York: John Wiley & Sons, Inc., 1952, pp. 142-143.

[15] L. K. Warne, W. A. Johnson, L. I. Basilio, W. L. Langston, and M. B. Sinclair, "Subcell Method For Modeling Metallic Resonators In Metamaterials," Progress In Electromagnetics Research B, Vol. 38, pp. 135-164, 2012.

[16] W. R. Smythe, **Static and Dynamic Electricity**, New York: Hemisphere Pub. Corp., 1989, pp.

123-124.

[17] E. C. Jordan and K. G. Balmain, **Electromagnetic Waves and Radiating Systems**, Englewood Cliffs, NJ: Prentice-Hall, Inc., 1968, Chapter 10, p. 485.

[18] M. Abramowitz and I. A. Stegun (editors), **Handbook of Mathematical Functions**, New York: Dover Pub., 1972, Inc., pp. 361, 485.

[19] L. Shen, T. T. Wu, and R. W. P. King, "A Simple Formula of Current in Dipole Antennas," IEEE Transactions on Antennas and Propagation, Vol. AP-16, No. 5, Sept. 1968.

[20] S. Tkachenko and J. Nitsch, "Investigation Of High-Frequency Coupling With Uniform And Non-Uniform Lines: Comparison Of Exact Analytical Results With Those Of Different Approximations," Proc. Int. Union. Radio Science XXVII General Assembly, Maastricht, The Netherlands, Aug. 7-24, 2002.

[21] R. W. King, **Transmission Line Theory**, New York: McGraw-Hill Book Co., 1955.

[22] L. A. Vaynshteyn, The Theory of Diffraction and the Factorization Method, Boulder, CO: The Golem Press, 1969, Ch. VI.

[23] R. G. Olsen and D. C. Chang, "Analysis of semi-infinite and finite thin-wire antennas above a dissipative earth," Radio Science, Vol. 11, No. 11, pp. 867-874, Nov. 1976.

[24] R. G. Olsen and D. C. Chang, "Electromagnetic Characteristics Of A Horizontal Wire Above A Dissipative Earth - Part III: Analysis Of Semi-Infinite And Finite-Thin Wire Antennas, Scientific Report No. 6, Electromagnetics Laboratory, Dept. of Electrical Engineering, U. of Colorado, Boulder, CO, Feb. 1974.

Intentionally Left Blank

Distribution

1	MS0492	K. C. Chen, 9411 (electronic copy)
1	MS0899	Technical Library, 9536 (electronic copy)
1	MS1033	O. Lavrova, 8812 (electronic copy)
1	MS1152	G. Pena, 1350 (electronic copy)
3	MS1152	S. Campione, 1352
1	MS1152	L. San Martin, 1352
1	MS1152	L. I. Basilio, 1352 (electronic copy)
1	MS1152	K. Cartwright, 1352 (electronic copy)
3	MS1152	L. K. Warne, 1352
1	MS1152	M. Halligan, 1353 (electronic copy)
1	MS1173	M. J. Walker, 5443 (electronic copy)
1	MS1173	L. D. Bacon, 5445 (electronic copy)
1	MS1177	J. P. Castro, 1355 (electronic copy)
1	MS1177	R. Shiek, 1355 (electronic copy)
1	MS9007	C. Lam, 8715 (electronic copy)


Sandia National Laboratories